© 2014 Haoyang Li

INVESTIGATION OF STABILITY AND ACCURACY OF HIGH ORDER GENERALIZED FINITE ELEMENT METHODS

BY

HAOYANG LI

THESIS

Submitted in partial fulfillment of the requirements
for the degree of Master of Science in Civil Engineering
in the Graduate College of the
University of Illinois at Urbana-Champaign, 2014

Urbana, Illinois

Adviser:

Professor Carlos Armando Duarte

ABSTRACT

The Generalized Finite Element methods (GFEMs) is a family of discretization methods which are based on the partition of unity (PoU) concept and are able to provide users with flexibility in choosing enrichments to approximate the target problem. The quality of the resulting approximation can be judged by the accuracy and its convergence rate, the conditioning and its growth rate. A major type of GFEM enrichment is the polynomial enrichment. Based on that, several modified versions of enrichments can be formulated and adopted in the simulation yielding different approximation behaviors in terms of accuracy and conditioning. By solving a one-dimensional problem and a two-dimensional problem, this report compares the numerical behaviors for different discretization methods including p-Lagrange FEM, p-hierarchical FEM, GFEM, stable GFEM (SGFEM) which is a recently proposed method with improved conditioning, and a number of variations on the GFEM and SGFEM. Other aspects considered are the linear dependency (LD) issue, the effect of mesh perturbation, and the factorization time. They are also presented to provide the reader with a broader knowledge of GFEMs.

To my parents, for their unconditional love and support.

ACKNOWLEDGEMENTS

First of all, I would like to express my gratitude to my advisor, Prof. C. Armando Duarte, for providing me with this opportunity to practice research in the field of the Generalized Finite Element method and related computational methods. His guidance and support not only helped me in the completion of this thesis but also nurtured me in the development of the skills and perspectives for future researches.

I would like to acknowledge my colleagues who offered me much help and encouragement. Additionally, I am grateful to all current and previous group members for their contributions to the researches in this group. All their works have laid a solid foundation for my own research.

I would like to thank the Department of Civil & Environmental Engineering at the University of Illinois at Urbana-Champaign for providing the resources helpful for conducting this project. And the partial support of this work by the Collaborative Center in Structural Sciences (C^2S^2) at the Ohio State University, sponsored by the U.S. Air Force Research Laboratory, Air Vehicles Directorate, is gratefully acknowledged.

Finally, of course, I am thankful to my friends and especially my family for their unconditionally support to all my efforts.

TABLE OF CONTENTS

LIST OF TABLES vii

LIST OF FIGURES ix

CHAPTER 1 INTRODUCTION 1

CHAPTER 2 ONE-DIMENSIONAL NUMERICAL EXPERIMENT 3

2.1 One-Dimensional Model Problem 3

2.2 Discretization Methods 5

2.3 General Information about Analysis Performed 7

2.4 1-D Numerical Experiments Results 11

2.5 Other aspects 18

2.6 Modifications on SGFEM 25

2.7 Summary for 1-D Numerical Experiments 36

CHAPTER 3 TWO-DIMENSIONAL NUMERICAL EXPERIMENT 37

3.1 Two-dimensional Model Problem 37

3.2 Discretization Methods for 2-D 38

3.3 2-D Numerical Experiments Results 40

3.4 Mesh perturbation 49

3.5 Numerical Expense: factorization time 53

3.6 Summary for 2-D Numerical Experiment 53

CHAPTER 4 CONCLUSIONS 56

REFERENCES 59

LIST OF TABLES

2.1 Number of DOFs for each method 20

2.2 First Few Eigenvalues for GFEM (*M3*) The multiplicity of zero eigenvalues is indicated in bracket unless it is equal to one 21

2.3 First Few Eigenvalues for GFEM w/o Linear Enrichment (*M4*) The multiplicity of zero eigenvalues is indicated in bracket unless it is equal to one 22

2.4 First Few Eigenvalues for SGFEM (*M5*) The multiplicity of zero eigenvalues is indicated in bracket unless it is equal to one 23

2.5 Patch Test - Solution Order = 2 24

2.6 Patch Test - Solution Order = 3 24

2.7 First Few Eigenvalues for SGFEM Mod1 (*M6*) The multiplicity of zero eigenvalues is indicated in bracket unless it is equal to one 27

2.8 First Few Eigenvalues for SGFEM Mod2 (*M7*) The multiplicity of zero eigenvalues is indicated in bracket unless it is equal to one 30

2.9 First Few Eigenvalues for SGFEM Mod3 (*M8*) The multiplicity of zero eigenvalues is indicated in bracket unless it is equal to one 33

2.10 First Few Eigenvalues for SGFEM Mod4 (*M9*) The multiplicity of zero eigenvalues is indicated in bracket unless it is equal to one 35

3.1 First few eigenvalues and the largest eigenvalues (indicated in square bracket) for FEM (*M1*) The multiplicity of zero eigenvalues is indicated in bracket unless it is equal to one 45

3.2 First few eigenvalues and the largest eigenvalues (indicated in square bracket) for GFEM (*M2*) The multiplicity of zero eigenvalues is indicated in bracket unless it is equal to one 46

3.3 First few eigenvalues and the largest eigenvalues (indicated in square bracket) for GFEM without linear enrichments (*M3*) The multiplicity of zero eigenvalues is indicated in bracket unless it is equal to one 47

3.4 First few eigenvalues and the largest eigenvalues (indicated in square bracket) for SGFEM (*M4*) The multiplicity of zero eigenvalues is indicated in bracket unless it is equal to one 48

LIST OF FIGURES

2.1 Manufactured solution for one-dimensional problem with $\alpha = 0.5$ and $x_b = 0.2$ . . . 4

2.2 Relative error in energy norm with respect to element size for p-Lagrange FEM (*M1*), p-Hierarchic FEM (*M2*), and GFEM (*M3*) . . . 13

2.3 SCN with respect to element size for p-Lagrange FEM (*M1*), p-Hierarchic FEM (*M2*), and GFEM (*M3*) . . . 13

2.4 Relative error in energy with respect to element size for GFEM (*M3*) and GFEM without linear enrichment (*M4*) . . . 15

2.5 SCN with respect to element size for p-Lagrange FEM (*M1*), GFEM (*M3*) and GFEM without linear enrichment (*M4*) . . . 15

2.6 Relative error in energy norm with respect to element size for SGFEM (*M5*) and GFEM without linear enrichment (*M4*) . . . 16

2.7 SCN with respect to element size for SGFEM (*M5*) and GFEM without linear enrichment (*M4*) . . . 16

2.8 Relative error in energy norm with respect to element size for p-Lagrange FEM (*M1*), p-Hierarchic FEM (*M2*), and SGFEM (*M5*) . . . 17

2.9 SCN with respect to element size for p-Lagrange FEM (*M1*), p-Hierarchic FEM (*M2*), and SGFEM (*M5*) . . . 17

2.10 Relative error in energy norm with respect to element size for GFEM (*M3*), SGFEM (*M5*), and SGFEM Mod1 (*M6*) . . . 26

2.11 SCN with respect to element size for GFEM (*M3*), SGFEM (*M5*), and SGFEM Mod1 (*M6*) . . . 26

2.12 Relative error in energy norm with respect to element size for GFEM (*M3*), SGFEM (*M5*), and SGFEM Mod2 (*M7*) . . . 29

2.13 SCN with respect to element size for GFEM (*M3*), SGFEM (*M5*), and SGFEM Mod2 (*M7*) . . . 29

2.14 Relative error in energy norm with respect to element size for GFEM (*M3*), SGFEM (*M5*), and SGFEM Mod3 (*M8*) 31

2.15 SCN with respect to element size for GFEM (*M3*), SGFEM (*M5*), and SGFEM Mod3 (*M8*) 32

2.16 Relative error in energy norm with respect to element size for GFEM (*M3*), SGFEM (*M5*), and SGFEM Mod4 (*M9*) 34

2.17 SCN with respect to element size for GFEM (*M3*), SGFEM (*M5*), and SGFEM Mod4 (*M9*) 34

3.1 Manufactured solution for two-dimensional problem 39

3.2 Relative error in energy norm with respect to element size for GFEM, GFEM without linear enrichments, SGFEM, and FEM in 2D 42

3.3 SCN with respect to element size for GFEM (*M2*), GFEM without linear enrichments (*M3*), SGFEM (*M4*), and FEM (*M1*) in 2D 43

3.4 SCN with respect to element size for GFEM (*M2*), GFEM without linear enrichments (*M3*), SGFEM (*M4*), and FEM (*M1*) in 2D for low p-order 43

3.5 Relative error in energy norm with respect to number of DOFs for GFEM (*M2*), GFEM without linear enrichments (*M3*), SGFEM (*M4*), and FEM (*M1*) in 2D . . . 44

3.6 SCN with respect to number of DOFs for GFEM (*M2*), GFEM without linear enrichments (*M3*), SGFEM (*M4*), and FEM (*M1*) in 2D 44

3.7 Relative error in energy norm with respect to SCN for GFEM (*M2*), GFEM without linear enrichments (*M3*), SGFEM (*M4*), and FEM (*M1*) in 2D 45

3.8 Relative error in energy norm with respect to element size for SGFEM (*M4*) and TRIA6 (*M1*) with perturbation parameter $\alpha = 0.3$ 50

3.9 Scaled condition number with respect to element size for SGFEM (*M4*) and TRIA6 (*M1*) with perturbation parameter $\alpha = 0.3$ 50

3.10 Relative error in energy norm with respect to DOFs for SGFEM (*M4*) and TRIA6 (*M1*) with perturbation parameter $\alpha = 0.3$ 51

3.11 Scaled condition number with respect to DOFs for SGFEM (*M4*) and TRIA6 (*M1*) with perturbation parameter $\alpha = 0.3$ 51

3.12 Distorted mesh 8x8 with $\alpha = 0.3$ 52

3.13 Error in energy norm with respect to LHS factorization time for TRIA6 (*M1*), GFEM (*M2*), and SGFEM (*M4*) 54

3.14 Error in energy norm with respect to total degrees of freedom for TRIA6 (*M1*), GFEM (*M2*), and SGFEM (*M4*) 54

CHAPTER 1

INTRODUCTION

In the context of engineering applications and research, the Generalized Finite Element method (GFEM) has a number of attractive features. GFEM can be treated as a meshless method. The key idea driving this method is the use of partition of unity (PoU) [1, 2, 3, 4], which is a set of functions whose values add up to the unity at each point in the problem domain. The *p*-GFEM formulation is one version of the GFEM family which is constructed by simply adding hierarchical enrichment to low order shape functions that satisfy PoU. Its advantages over traditional finite element methods (FEM) are discussed by Duarte et al. [5] and Oden et al. [1]. The method delivers higher rates of convergence, generates smaller system of equations leading to less computational effort, enables easier implementation for Dirichlet boundary conditions, and allows pre-constructed approximation space based on *a priori* knowledge of the solution. Recently Kim and Bathe proposed the cover scheme which is basically the same as GFEM. [6]. They stated that their scheme could improve the accuracy of solutions as compared to FEM. Also, the scheme is computationally effective and able to improve solutions when elements are distorted.

Despite the fact that GFEM has several excellent properties such as high accuracy and fast convergence, there are also issues that limit the efficiency of the method in its application to engineering practices. One important issue is the Linear Dependency (LD) problem: even in a well-posed boundary value problem (BVP), the number of unknowns is greater than the number of linear independent shape functions in the constructed approximation. In terms of *p*-GFEM, the LD issue arises when all nodes are enriched with the same number and order of enrichments. As discussed by Tian et al. [7, 8] and An et al. [9, 10], this issue will introduce spurious zero eigenvalues meaning singular stiffness matrix and rank deficiency of the system. The LD will also lead to bad conditioning when the enrichment order is increased or mesh is refined because the smallest nonzero eigenvalue is getting closer to zero because of the nearly linear dependency between some basis functions. A high condition number will then significantly affect the round off error of the solution. A theoretical derivation of the rate of growth in condition number is performed by Li et al. [11], which shows the condition number grows fast for standard GFEM when decreasing element size. In [7], a simple fix to LD problem is proposed: that is to set proper constraints on some

extra degrees of freedom (DOF). A new PoU-based three-node triangle element that also deals with the LD problem developed by Cai et al. can be found in [12]. Another approach to handle the LD problem is known as the Stable Generalized finite element method (SGFEM). This method was proposed recently by Babuška and Banerjee [13]. SGFEM mainly focuses on stabilizing the condition number of the stiffness matrix. It also successfully eliminates the spurious zero eigenvalues, namely fixing the LD issue. Properties and behavior of higher order SGFEM is investigated further by Zhang et al. [14]. SGFEM can yield a high order of convergence rate similar to GFEM and much better conditioning in contrast to standard GFEM. The concept of SGFEM can actually be applied to not only polynomial enrichments but also to any type of enrichments. In [15], Gupta et al. shows that the ill conditioning of GFEM with singular enrichments can be fixed by SGFEM and the accuracy can also be improved.

Both bad conditioning and the LD problem will lead to singular or nearly stiffness matrix. In this thesis, Neumann boundary conditions are used for the boundary value problems (BVPs). Therefore, the stiffness matrix is singular due to rigid body motions. Hence, we need an effective way to handle singular systems. Two approaches: matrix pseudo-inverse and Babuška algorithm are described in Section 2.3.2. Illustration of Babuška algorithm can also be found in [5].

This thesis investigates the accuracy and conditioning of FEM, GFEM, and SGFEM as well as other related aspects based on analysis results. In Chapter 2, a one-dimensional boundary value problem (BVP) is solved with different discretization methods. The GFEM and SGFEM with higher order enrichments are also adopted to study their accuracy and stability. In Chapter 2 Sections 2.3.3 and 2.5.2, the total degrees of freedom and number of zero eigenvalues of the stiffness matrix are compared between methods. Additionally, a set of patch tests is performed to make connections between the enrichment order and the order of accuracy. In Section 2.6, in addition to standard methods, we investigate four modified versions of the SGFEM in order to further understand the method. In Chapter 3, we extend the BVP to a two-dimensional problem in order to study whether the methods behave in similar ways for 2-D as for 1-D. In Sections 3.4 and 3.5, analysis under mesh perturbation and factorization time are discussed briefly. At the end of both Chapters 2 and 3, summaries of comments drawn from 1-D and 2-D numerical experiments are given. Finally, in Chapter 4, major conclusions of the study are stated.

CHAPTER 2

ONE-DIMENSIONAL NUMERICAL EXPERIMENT

2.1 One-Dimensional Model Problem

The one-dimensional numerical experiments presented in this report are based on the Neumann Boundary Value Problem (BVP) defined below.

The governing equation reads

$$-\frac{d^2u}{dx^2} = T(x) \qquad x \in [0,\, 1] \tag{2.1}$$

It is noted that this problem can be interpreted as a bar with EA equaling unity for convenience.

The Neumann BCs are defined as

$$\frac{du}{dx}(0) = f_0; \quad \frac{du}{dx}(1) = f_1 \tag{2.2}$$

The manufactured solution of BVP above is taken as

$$u(x) = (1-x)(\arctan(\alpha(x-x_b)) + \arctan(\alpha x_b)) \tag{2.3}$$

where $x_b = 0.2$ and $\alpha = 0.5$.

This manufactured solution is a smooth function that is shown in Figure 2.1.

Body force $T(x)$ is given by plugging the solution into (2.1), which reads

$$T(x) = \frac{2\alpha}{1+\alpha^2(x-x_b)^2} + \frac{2(1-x)\alpha^3}{(1+\alpha^2(x-x_b)^2)^2}(x-x_b) \tag{2.4}$$

and the traction boundary conditions can be calculated using (2.3) and applied according to (2.2).

The exact strain energy is given by

$$U_{exact} = \frac{1}{2}\int_0^1 \frac{du}{dx}\frac{du}{dx}dx = 0.04087775479380799 \tag{2.5}$$

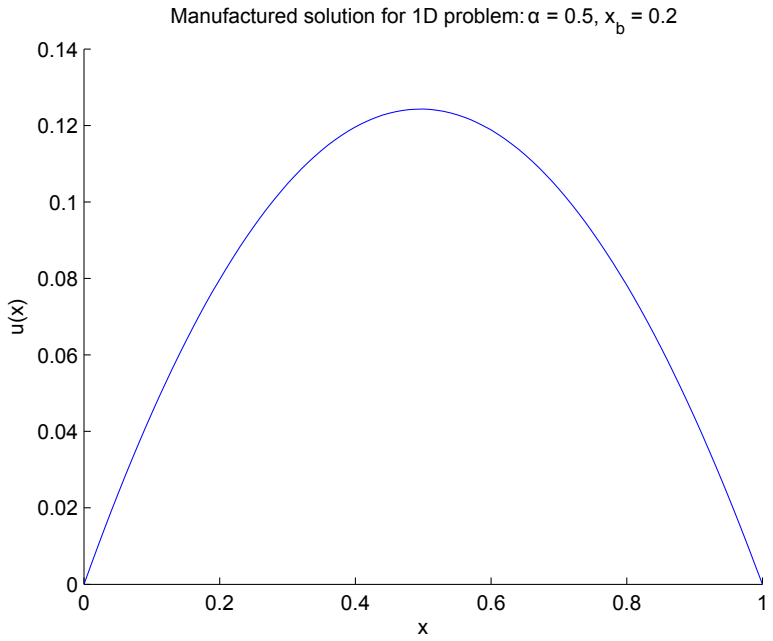


Fig. 2.1 Manufactured solution for one-dimensional problem with $\alpha = 0.5$ and $x_b = 0.2$

2.2 Discretization Methods

The nine discretization methods described below are investigated for the 1-D case. All enrichments added for GFEM and SGFEM are polynomial enrichments. And all nodes are enriched with the same order of polynomials in GFEM and SGFEM.

M1. p-Lagrange FEM: standard FEM with Lagrange shape functions.

M2. p-Hierarchical FEM: FEM with its basis created by Legendre polynomials [16].

M3. Standard GFEM with complete enrichment:

The enrichment and the resulting shape functions for *M3* read

$$\mathcal{L}_\alpha^p = (\frac{x - x_\alpha}{h})^p \tag{2.6}$$

$$\phi_\alpha = \varphi_\alpha \times \{1, \mathcal{L}_\alpha^1, \mathcal{L}_\alpha^2, \mathcal{L}_\alpha^3, ..., \mathcal{L}_\alpha^p\} \tag{2.7}$$

where φ_α is the linear PoU function at node α (i.e., the linear Lagrange shape function) and ϕ_α is the GFEM shape function at node α after enrichment. Formulations for the following discretization methods share the same notation of φ_α and ϕ_α.

M4. GFEM without linear enrichment:

The enrichment for *M4* is constructed in the same way as *M3* except that the linear enrichment term is dropped. The resulting shape functions for *M4* reads

$$\phi_\alpha = \varphi_\alpha \times \{1, \mathcal{L}_\alpha^2, \mathcal{L}_\alpha^3, ..., \mathcal{L}_\alpha^p\} \tag{2.8}$$

where $\mathcal{L}_\alpha^p$ is as defined in (2.6).

M5. Standard SGFEM:

The enrichment and the resulting shape functions for *M5* are given by

$$\hat{\mathcal{L}}_\alpha^p = \mathcal{L}_\alpha^p - \mathcal{I}_{\omega_\alpha}(\mathcal{L}_\alpha^p) \tag{2.9}$$

$$\phi_\alpha = \varphi_\alpha \times \{1, \hat{\mathcal{L}}_\alpha^2, \hat{\mathcal{L}}_\alpha^3, ..., \hat{\mathcal{L}}_\alpha^p\} \tag{2.10}$$

where $\mathcal{I}_{\omega_\alpha}(\mathcal{L}_\alpha^p)$ denotes the piecewise linear finite element interpolant [13] of the enrichment function $\mathcal{L}_\alpha^p$ which is defined in (2.6).

M6. Modified SGFEM with linear enrichment not subtracting FE interpolant (SGFEM Mod1):

The enrichment for *M6* is constructed in a similar way as *M5* except that one linear term is added in the set of enrichments. The resulting shape functions for *M6* is then given by

$$\phi_\alpha = \varphi_\alpha \times \{1, \mathcal{L}^1_\alpha, \hat{\mathcal{L}}^2_\alpha, \hat{\mathcal{L}}^3_\alpha, ..., \hat{\mathcal{L}}^p_\alpha\} \tag{2.11}$$

where $\mathcal{L}^p_\alpha$ and $\hat{\mathcal{L}}^p_\alpha$ are as defined in (2.6) and (2.9), respectively.

M7. Modified SGFEM with linear enrichment not subtracting FE interpolant and without quadratic enrichment(SGFEM Mod2):

The enrichment for *M7* is constructed in the same way as *M6* except that the quadratic term is dropped. The resulting shape functions for *M7* is then given by

$$\phi_\alpha = \varphi_\alpha \times \{1, \mathcal{L}^1_\alpha, \hat{\mathcal{L}}^3_\alpha, ..., \hat{\mathcal{L}}^p_\alpha\} \tag{2.12}$$

where $\mathcal{L}^p_\alpha$ and $\hat{\mathcal{L}}^p_\alpha$ are as defined in (2.6) and (2.9), respectively.

M8. SGFEM without shifting or scaling of enrichments(SGFEM Mod3):

The enrichment for *M8* is constructed in a similar way as *M5* except that no shifting and scaling are applied to polynomial enrichments. The enrichment and the resulting shape functions for *M8* read

$$\bar{\mathcal{L}}^p_\alpha = x^p \tag{2.13}$$

$$\hat{\bar{\mathcal{L}}}^p_\alpha = \bar{\mathcal{L}}^p_\alpha - \mathcal{I}_{\omega_\alpha}(\bar{\mathcal{L}}^p_\alpha) \tag{2.14}$$

$$\phi_\alpha = \varphi_\alpha \times \{1, \hat{\bar{\mathcal{L}}}^2_\alpha, \hat{\bar{\mathcal{L}}}^3_\alpha, ..., \hat{\bar{\mathcal{L}}}^p_\alpha\} \tag{2.15}$$

where $\hat{\bar{\mathcal{L}}}^p_\alpha$ is the enrichment at node α after subtracting the piecewise linear FE interpolant $\mathcal{I}_{\omega_\alpha}(\bar{\mathcal{L}}^p_\alpha)$ of the enrichment function $\bar{\mathcal{L}}^p_\alpha$.

M9. SGFEM without scaling of enrichments(SGFEM Mod4):

The enrichment for *M9* is constructed in a similar way as *M8* except that the shifting is used. The enrichment and the resulting shape functions are then given by

$$\tilde{\mathcal{L}}^p_\alpha = (x - x_\alpha)^p \tag{2.16}$$

$$\hat{\tilde{\mathcal{L}}}^p_\alpha = \tilde{\mathcal{L}}^p_\alpha - \mathcal{I}_{\omega_\alpha}(\tilde{\mathcal{L}}^p_\alpha) \tag{2.17}$$

$$\phi_\alpha = \varphi_\alpha \times \{1, \hat{\tilde{\mathcal{L}}}^2_\alpha, \hat{\tilde{\mathcal{L}}}^3_\alpha, ..., \hat{\tilde{\mathcal{L}}}^p_\alpha\} \tag{2.18}$$

where $\hat{\tilde{\mathcal{L}}}^p_\alpha$ is the enrichment at node α after subtracting the piecewise linear FE interpolant $\mathcal{I}_{\omega_\alpha}(\tilde{\mathcal{L}}^p_\alpha)$ of the enrichment function $\tilde{\mathcal{L}}^p_\alpha$.

Methods *M1* through *M5* are the original options for the one-dimensional experiments. Methods *M6* and *M7* were brought up after studying the results of *M1* through *M5*. Detailed results and the reasons why we came up with these two methods will be illustrated in Section 2.6 after discussion of the original ones. The study of methods *M7* and *M8* are performed for a comprehensive view of the SGFEM formulation.

2.3 General Information about Analysis Performed

2.3.1 Notation Adopted

Notation about the approximation order is illustrated below. This clarification will help in understanding the resulting plots and discussion in following sections.

For p-Lagrange FEM, pBar2, pBar3, and pBar4 indicate 1-D bar elements with 2, 3, and 4 nodes respectively, which correspond to linear, quadratic, and cubic shape functions respectively.

For p-Hierarchical FEM, n is the order of Legendre Polynomial being used for element shape functions.

For GFEM and SGFEM, p is the order of enrichment. Therefore, the linear PoU always corresponds to $p = 0$.

2.3.2 Methods to deal with singular matrices

Since the one-dimensional model problem presented in this chapter and the two-dimensional model that will be introduced in Chapter 3 are both subject to Neumann boundary conditions, rigid body motions are not prevented. Thus the resulting stiffness matrix will have zero eigenvalues which means the matrix is singular. Additionally, the LD issue mentioned in Chapter 1 will also introduce zero eigenvalues. Solving a singular system requires non-trivial effort. Therefore two computational methods are adopted to deal with this issue: the matrix pseudo-inverse method and Babuška algorithm.

Moore-Penrose pseudo-inverse of matrix: The pseudo-inverse of a singular matrix is used for solving the one-dimensional problem. This method is a Matlab function of which syntax is `x = pinv(A)*b` to solve the singular system $\mathbf{Ax} = \mathbf{b}$. When solving in this way, the computation is based on the Singular Value Decomposition(SVD) of $\mathbf{A}$, and any singular values less than default tolerance are treated as zero. The default tolerance in Matlab is computed by `MAX(SIZE(A)) * NORM(A) * EPS(class(A))` which in our problem is roughly smaller than 10^{-12}.

Babuška Algorithm: Babuška algorithm is an iterative algorithm used to solve singular systems [5]. It is adopted to solve our two-dimensional problem. To illustrate this algorithm, assume we are to solve the system of equations

$$\tilde{\mathbf{K}}\tilde{\mathbf{u}} = \tilde{\mathbf{f}} \tag{2.19}$$

where $\tilde{\mathbf{K}}$ is a positive semi-definite stiffness matrix having zero eigenvalues. Since the perturbation parameter is better to be fixed no matter what the scale of the stiffness matrix is, the stiffness matrix is firstly scaled in the following manner

$$\mathbf{K} = \mathbf{T}\tilde{\mathbf{K}}\mathbf{T}, \quad \mathbf{u} = \mathbf{T}^{-1}\tilde{\mathbf{u}}, \quad \mathbf{f} = \mathbf{T}\tilde{\mathbf{f}} \tag{2.20}$$

where the scaling matrix reads

$$T_{ij} = \frac{\delta_{ij}}{\sqrt{\tilde{K}_{ij}}} \tag{2.21}$$

Then the system of equations in terms of the scaled matrix is given by

$$\mathbf{Ku} = \mathbf{f} \tag{2.22}$$

The above modification transfers $\tilde{\mathbf{K}}$ into a scaled matrix $\mathbf{K}$ with unit diagonal entries. Then we do perturbation on $\mathbf{K}$ as follows

$$\mathbf{K}_\varepsilon = \mathbf{K} + \varepsilon\mathbf{I} \tag{2.23}$$

where ε is a small positive parameter and $\mathbf{I}$ is the identity matrix of the same size as $\mathbf{K}$. The perturbed stiffness matrix $\mathbf{K}_\varepsilon$ becomes non-singular. Then the solution $\mathbf{u}$ to the perturbed system can be computed by

$$\mathbf{u_0} = \mathbf{K}_\varepsilon^{-1}\mathbf{f} \tag{2.24}$$

The expression of the residual reads

$$\mathbf{r_0} = \mathbf{f} - \mathbf{K}\mathbf{u_0} \tag{2.25}$$

Let the error between solutions to the original system and the perturbed system reads

$$\mathbf{e_0} = \mathbf{u} - \mathbf{u_0} \tag{2.26}$$

Assume that the perturbed matrix is almost identical to the unperturbed one. Then we have

$$\mathbf{K}_\varepsilon \mathbf{e_0} \approx \mathbf{K}\mathbf{e_0} = \mathbf{K}\mathbf{u} - \mathbf{K}\mathbf{u_0} = \mathbf{r_0} \tag{2.27}$$

Therefore, the error can be expressed as

$$\mathbf{e_0} = \mathbf{K}_\varepsilon^{-1}\mathbf{r_0} \tag{2.28}$$

Do the following iteration

$$\mathbf{r_i} = \mathbf{e_0} - \sum_{\mathbf{j=0}}^{\mathbf{i-1}} \mathbf{K}\mathbf{e_j}, \quad \mathbf{e_i} = \mathbf{K}_\varepsilon^{-1}\mathbf{r_i}, \quad \mathbf{u_i} = \mathbf{u_0} + \sum_{\mathbf{j=0}}^{\mathbf{i-1}} \mathbf{e_j} \tag{2.29}$$

until the quantity

$$\left| \frac{\mathbf{e_i}\mathbf{K}\mathbf{e_i}}{\mathbf{u_i}\mathbf{K}\mathbf{u_i}} \right| \tag{2.30}$$

is smaller than the tolerance value set by the user. Finally, the solution to the original system is given by

$$\tilde{\mathbf{u}} = \mathbf{T}\mathbf{u} \tag{2.31}$$

In our computations, the perturbation parameter ε is set to 10^{-12}, and tolerance for iteration stopping criteria is set to 10^{-12}.

2.3.3 Computation of Eigenvalues and Scaled Condition Number

For both one-dimensional and two-dimensional problems, a stiffness matrix is first formed. The scaled stiffness matrix is then given by

$$\bar{K}_{ij} := \frac{K_{ij}}{\sqrt{K_{ii}}\sqrt{K_{jj}}} \tag{2.32}$$

Eigenvalues of the stiffness matrices are computed using Matlab functions `eigs(`$\bar{K}$`,1)` and `eigs(`$\bar{K}$`,n,'sm')` for conditioning study. The first function returns the largest scaled eigenvalue. The second function returns n nonzero eigenvalues closest to zero. The scaled condition number (SCN) is then defined as

$$SCN = \frac{\sigma_{max}(\bar{\mathbf{K}})}{\sigma_{min}(\bar{\mathbf{K}})} \tag{2.33}$$

where σ_{max} and σ_{min} are the largest and the smallest singular values of the scaled matrix, respectively.

In computing scaled condition numbers of the stiffness matrix, a cut-off value of 10^{-13} is set for identifying zero eigenvalues and for picking the smallest non-zero eigenvalues. Thus any eigenvalue smaller than this tolerance is treated as zero. Then the condition number is given by the ratio of the largest eigenvalue and the smallest non-zero ones.

2.4 1-D Numerical Experiments Results

In this section, methods *M1* through *M5* will be compared according to four groupings. Analysis results are mainly focused on accuracy and conditioning.

Accuracy is measured by the relative error in the energy norm which reads

$$e_r(u)_E = \sqrt{\frac{|U_{\text{approx}} - U_{\text{exact}}|}{|U_{\text{exact}}|}} \tag{2.34}$$

where U_{approx} and U_{exact} are the strain energy of the approximate and exact solutions, respectively.

The conditioning is measured by the Scaled Condition Number (SCN) which is defined in Section 2.3.3.

During the experiments, we find that the lower limit of the error in energy norm is around 10^{-7}. Beyond that point, errors may be affected by the machine precision, and curves may not converge as expected. Because of this observation, in the following plots, we didn't include curves of some high order formulations. The curves we pick can adequately represent the behavior of the methods and illustrate our points.

2.4.1 Group 1: *p*-Lagrange FEM, *p*-Hierarchic FEM, and GFEM

Within this group, we compare GFEM with two commonly used methods in engineering practice that are *p*-Lagrange FEM and *p*-Hierarchical FEM. The latter one (*M2*) is known for its good accuracy and conditioning, while the former one (*M1*) provides good accuracy but worse conditioning as the polynomial order increases. In [17], Kim et al. theoretically showed the growth rate of condition numbers for *p*-FEM.

Curves for $e_r(u)_E$ and the scaled condition number with respect to element size are plotted in Figures 2.2 and 2.3, from which we can observe accuracy, conditioning, and convergence rate for methods *M1*-*M3*.

From Figure 2.2, error curves for the same order of shape functions for all three methods are on top of each other. This shows that *p*-Lagrange FEM, *p*-Hierarchic FEM, and GFEM with complete polynomial enrichment deliver exactly the same level of accuracy in the one-dimensional case.

The slopes, which in our plots are indicated as β, in error plots represent the convergence rates

for each choice of method. From the theory of *a priori* error estimate[18, 16], it is known that the optimal convergence rates are controlled by the order of FEM approximation. For the problem with smooth solution which is the case for this BVP, the optimal convergence rates are equal to the order of FE shape functions. For GFEM, we observe that convergence rates are equal to the order of enrichments plus 1, that is $\beta = p+1$ which is the order of the resulting polynomials for approximation. By refining the mesh, we keep getting closer to the optimal convergence rate for errors in the energy norm as expected.

The slopes denoted by β in SCN plots represent the rate of growth in SCNs with respect to element size h. Figure 2.3 shows that p-Lagrange FEM yields larger SCN when we increase the order of the approximation. For each of its curves, it shows a growth in the SCN of order h^{-2}. As for p-Hierarchical FEM, it gives the best conditioning among all three methods. It shows a growth in the SCN of order h^{-2}, with no difference between different orders of shape functions.

The conditioning for the GFEM with linear enrichment ($p = 1$) is exactly the same as that for linear p-Hierarchical FEM. Note that GFEM with linear enrichment delivers quadratic convergence rates in the energy norm, as shown in Figure 2.2. This shows that the GFEM with linear enrichments (*M3*) is as accurate as *quadratic* p-Lagrange and p-Hierarchic FEM, while having the same SCN as the p-Hierarchic FEM. This property leads the idea of constructing modified SGFEM discretizations in Section 2.6. However, the GFEM with quadratic enrichment ($p = 2$) has an SCN that asymptotically grows as h^{-4}, while being as accurate as cubic p-Lagrange and cubic p-Hierarchic FEM.

SCNs of p-Hierarchic FEM are always the smallest for all three methods. By comparing p-Lagrange and GFEM, we observe that the curve for GFEM with $p = 1$ is always below the curve for quadratic p-Lagrange FEM. For GFEM with $p = 2$, its scaled condition numbers are smaller than those of p-Lagrange FEM when $h = 2$, 4, and 8 (i.e., coarse meshes), but are larger when solving on finer meshes due to the larger growth rate in the SCN.

2.4.2 Group 2: GFEM with Complete Enrichment and GFEM without Linear Enrichment

Within this group, we are aiming to find how the accuracy and conditioning behave if the linear enrichment is skipped. We compare the performance of discretization methods *M3* and *M4*.

The plot for relative error in energy norm (Figure 2.4) shows that it yields larger errors if the linear enrichment is skipped. For GFEM without linear enrichment (*M4*), convergence rates are equal

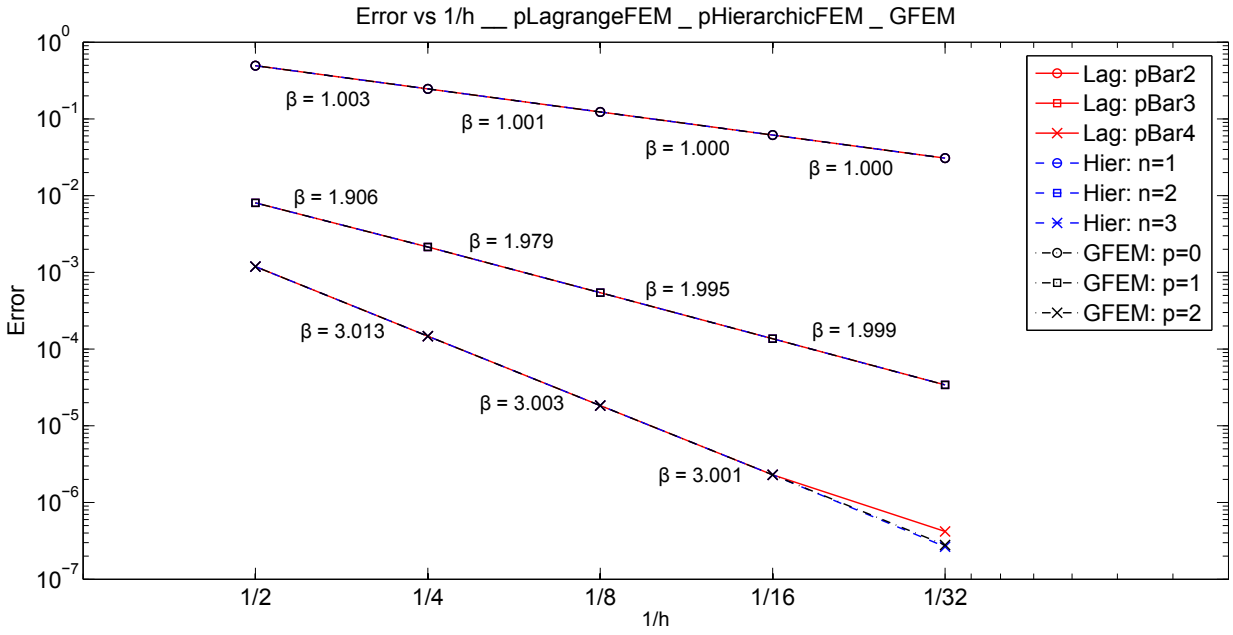


Fig. 2.2 Relative error in energy norm with respect to element size for *p*-Lagrange FEM (*M1*), *p*-Hierarchic FEM (*M2*), and GFEM (*M3*)

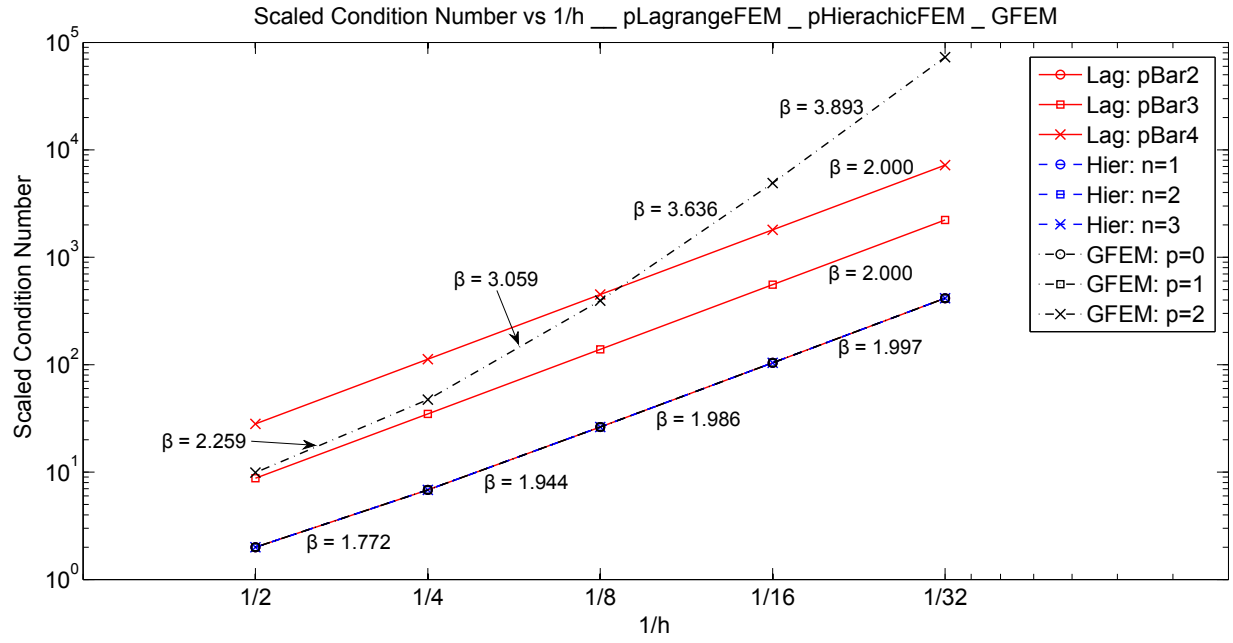


Fig. 2.3 SCN with respect to element size for *p*-Lagrange FEM (*M1*), *p*-Hierarchic FEM (*M2*), and GFEM (*M3*)

to two for $p = 2$ and three for $p = 3$. The quadratic enrichment do not provide cubic convergence which is the case for GFEM with complete enrichment. Thus, instead of $\beta = p + 1$ for standard GFEM (*M3*), we have the rate of convergence $\beta = p$ (i.e. the order of the enrichment) for GFEM with no linear enrichment. Another observation is that the error for method *M4* suddenly becomes higher when we refine the mesh from $h = 2$ to $h = 4$ with $p = 2$. This issue will be discussed in Section 2.5.

Figure 2.5 shows that although the accuracy and convergence rate are deteriorated, the conditioning gets much better for GFEM without linear enrichment. The plot shows that the conditioning is nearly constant for coarse meshes and high p-order. Then it shows a growth in the SCN of order h^{-2} with further mesh refinement. This fact illustrates that by skipping the linear enrichment the linear dependency issue is fixed for low p-order. For high p-order and coarse meshes (e.g., $p = 4$, $h = 2$), as it will be shown in Section 2.5.1, there is still one spurious zero eigenvalue which denotes the LD issue.

If we add p-Lagrange FEM into the conditioning comparison, we find that: for $p = 2$, GFEM without linear enrichment (*M4*) always has better conditioning than p-Lagrange FEM; for $p = 3$, *M4* provides better conditioning than p-Lagrange FEM except for the coarsest mesh.

If we recall that conditioning curves for p-Hierarchic FEM are all below the curves for p-Lagrange FEM, we can conclude that the higher the enrichment order we adopt in the GFEM (*M4*), the finer the mesh has to be so that GFEM without linear enrichment can have the same conditioning as p-Hierarchic FEM.

2.4.3 Group 3: SGFEM and GFEM without Linear Enrichment

Since the GFEM without linear enrichment (*M4*) offers more stable conditioning, standard SGFEM (*M5*) should be put into the comparison with *M4* to attain an idea of their approximation qualities and the effect of the linear FE interpolant $\mathcal{I}_{\omega_\alpha}(\mathcal{L}_\alpha^p)$. After all, the only difference between *M4* and *M5* is whether $\mathcal{I}_{\omega_\alpha}(\mathcal{L}_\alpha^p)$ is subtracted from each enrichment.

From Figures 2.6 and 2.7, we find that the SGFEM (*M5*) gives higher accuracy than the GFEM without linear enrichment (*M4*). Convergence rates for both methods are nearly identical, which are equal to the order of the enrichment (i.e., $\beta = p$) as discussed earlier. The conditioning curves for both methods behave in the similar manner. For p-order higher than two, SGFEM yields higher SCN than *M4* within the flat region of the curves.

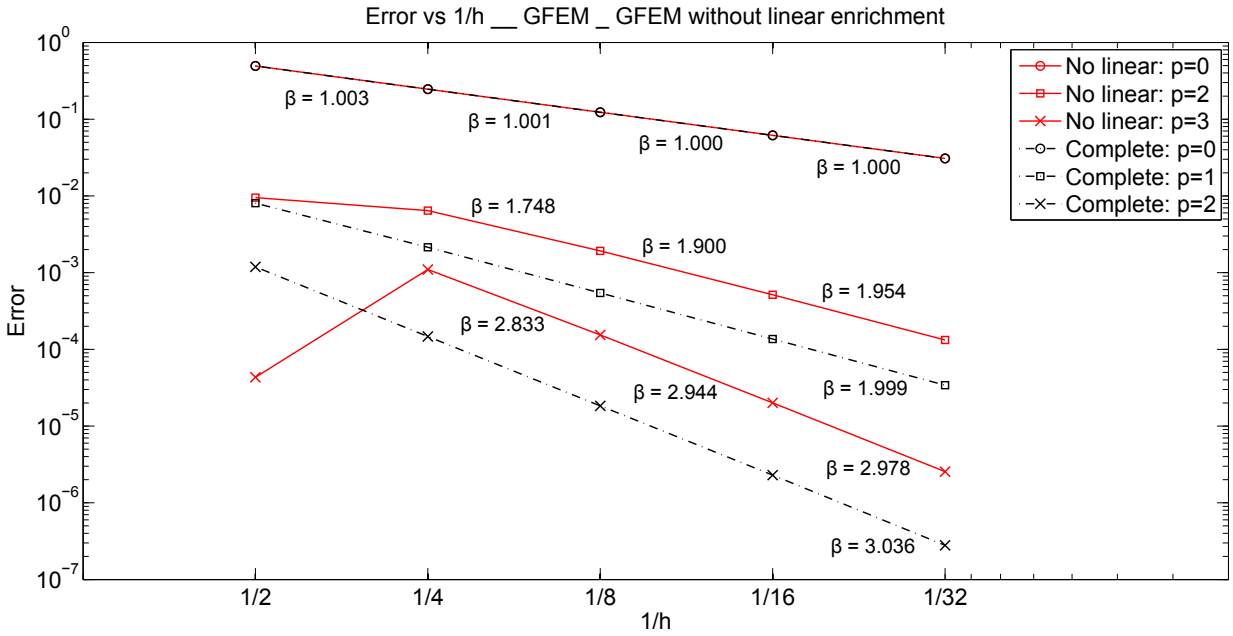


Fig. 2.4 Relative error in energy with respect to element size for GFEM (*M3*) and GFEM without linear enrichment (*M4*)

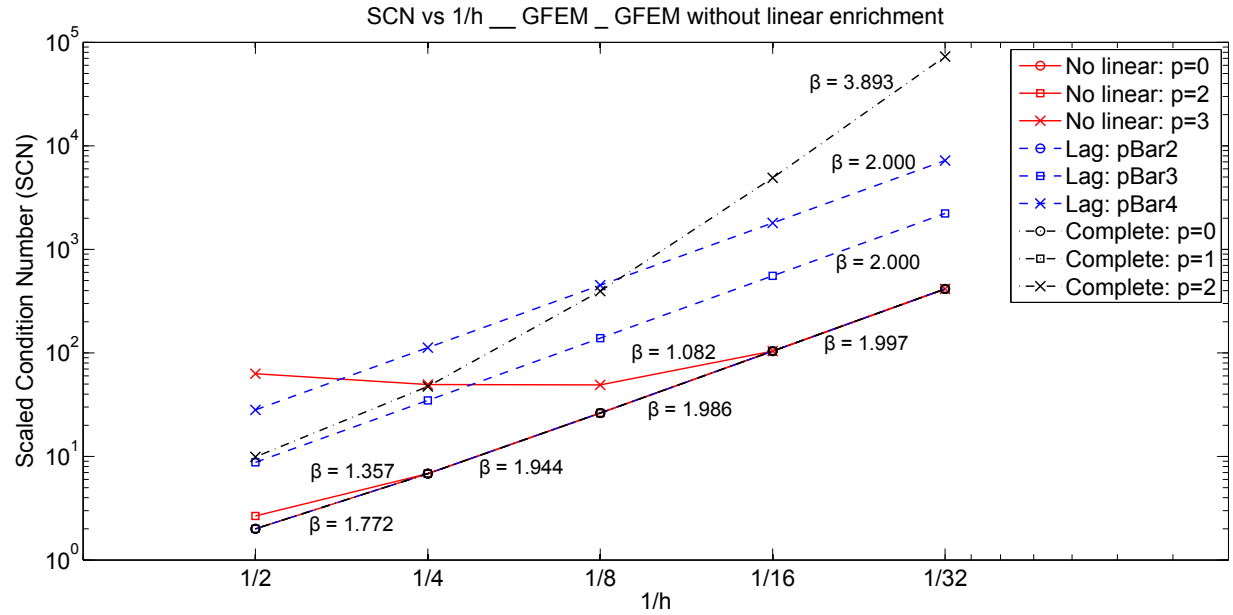


Fig. 2.5 SCN with respect to element size for *p*-Lagrange FEM (*M1*), GFEM (*M3*) and GFEM without linear enrichment (*M4*)

2.4.4 Group 4: *p*-Lagrange FEM, *p*-Hierarchic FEM, and SGFEM

Although we have shown in the previous section that the SGFEM (*M5*) gives better accuracy than the GFEM without linear enrichment (*M4*), Figure 2.8 shows that the SGFEM is of lower accuracy

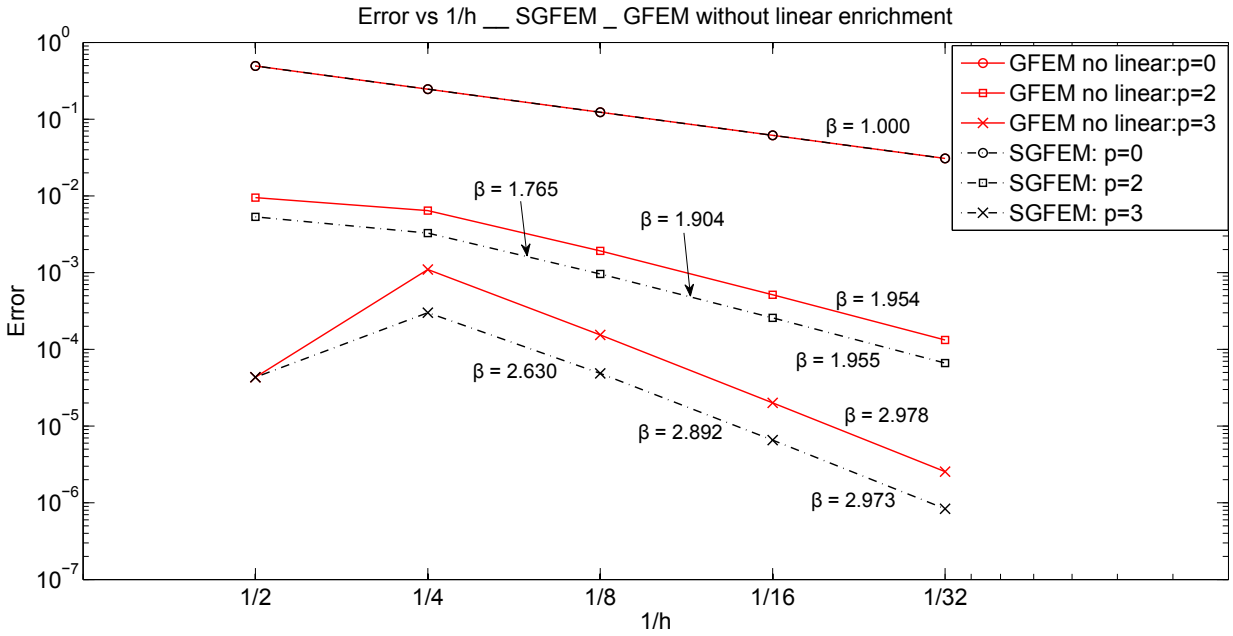


Fig. 2.6 Relative error in energy norm with respect to element size for SGFEM (*M5*) and GFEM without linear enrichment (*M4*)

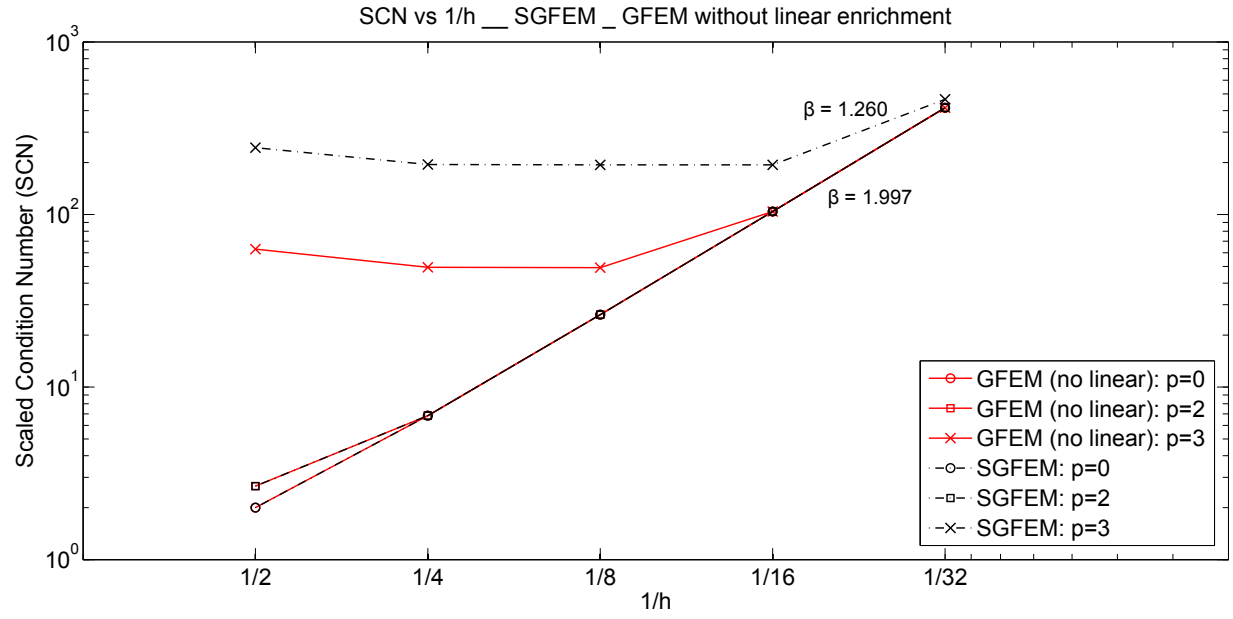


Fig. 2.7 SCN with respect to element size for SGFEM (*M5*) and GFEM without linear enrichment (*M4*)

than the FEM.

In terms of conditioning, *p*-Hierarchical FEM gives best conditioning for any polynomial order. SCN curves for SGFEM asymptotically approach the curves for *p*-Hierarchical FEM. SCNs of

SGFEM for $p = 2$ are always smaller than quadratic p-Lagrange FEM. And SCNs of SGFEM for $p = 3$ are smaller than cubic p-Lagrange FEM except for coarse meshes $h = 2$ and 4.

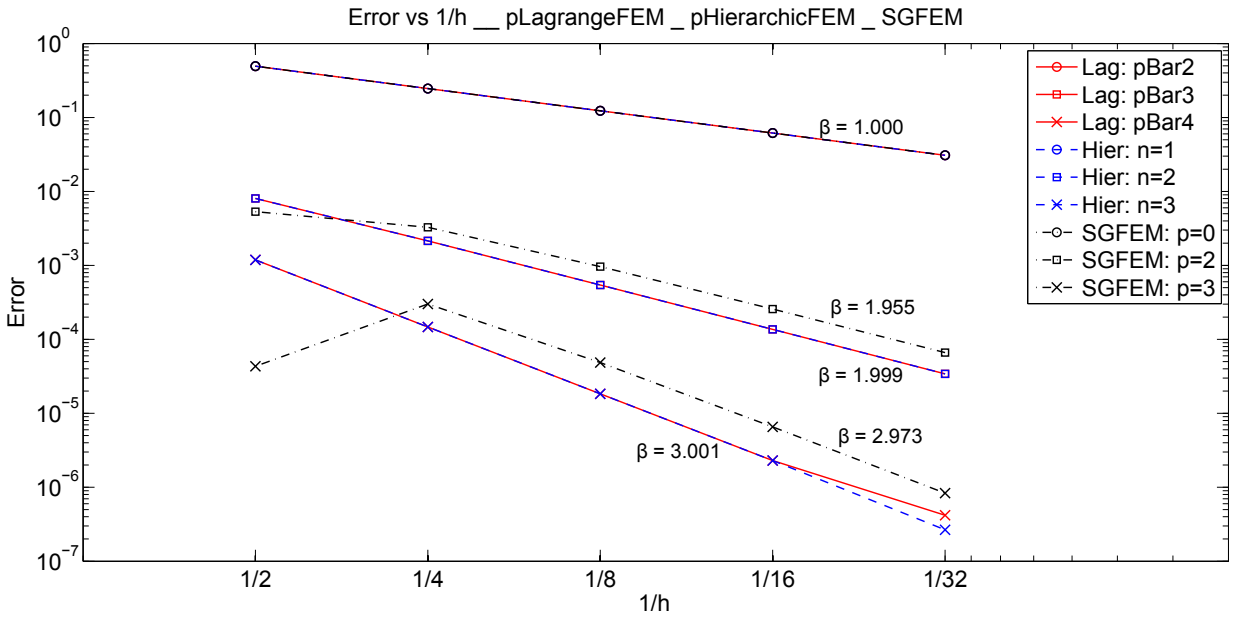


Fig. 2.8 Relative error in energy norm with respect to element size for p-Lagrange FEM (*M1*), p-Hierarchic FEM (*M2*), and SGFEM (*M5*)

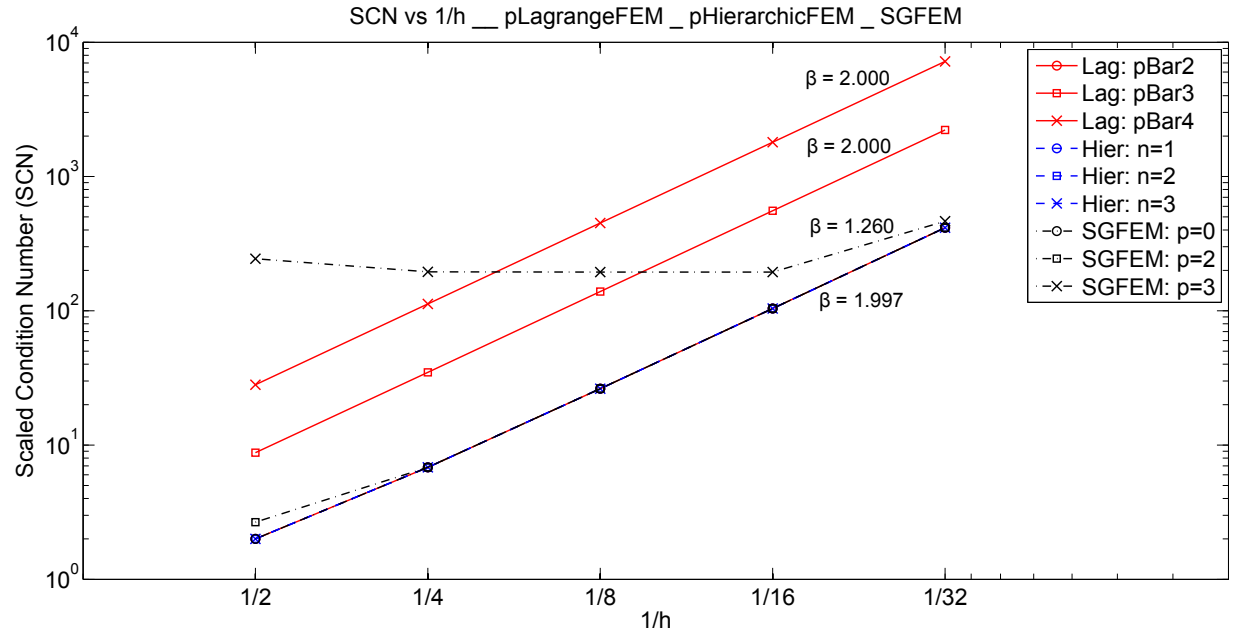


Fig. 2.9 SCN with respect to element size for p-Lagrange FEM (*M1*), p-Hierarchic FEM (*M2*), and SGFEM (*M5*)

2.5 Other aspects

In Section 2.4, we discussed the results in terms of the accuracy and conditioning for each method. This section presents other aspects which explicitly refer to the number of DOFs, the number of zero eigenvalues, and the results for some simple patch tests. The total number of DOFs and the number of zero eigenvalues are related to the LD issue. The patch tests are performed to check the approximation order of methods.

2.5.1 Number of DOFs and zero eigenvalues

With Table 2.1, we can compare the number of DOFs of the resulting system for each case. Tables 2.2, 2.3, and 2.4 show the first few smallest nonzero eigenvalues associated with stiffness matrices for GFEM, GFEM without linear enrichment, and SGFEM and indicate the number of zero eigenvalues each method yields.

The first few smallest nonzero eigenvalues can be treated as another measure to the conditioning of the matrix. For standard GFEM, the orders of the magnitude of the first few eigenvalues decrease rapidly. On the other hand, the orders of the magnitude of the eigenvalues tabulated for SGFEM and GFEM without linear enrichment remain stable as the mesh is refined. This observation matches the SCN behaviors for *M3-M5* in Section 2.4.

Since the Neumann boundary conditions are used for our 1-D problem, necessarily, the stiffness matrix for FEM has one zero eigenvalue representing the rigid body motion. As we can see, GFEM with complete enrichment always has more DOFs than FEM for the same mesh. This fact leads the stiffness matrix constructed by GFEM to have more than one zero eigenvalue. The number of zero eigenvalues is however independent of the element size. In fact, the number of zero eigenvalues is equal to the difference in the number of DOFs between FEM and other methods plus one. It can be easily shown that in our case in which all nodes are enriched with the same enrichment functions, the difference in DOFs is equal to the enrichment order p. Thus, the number of zero eigenvalues is equal to $p+1$. GFEM without linear enrichment and SGFEM always have the same number of DOFs, and for finer meshes or lower p-order, they have less DOFs than FEM. They yield only one zero eigenvalue in most cases, which corresponds to the rigid body motion of the bar. In other words, we decrease the number of DOFs and get rid of the spurious modes by skipping the linear enrichment. We can simply calculate the number of spurious zero eigenvalues using

$$N_{spurious\ zeros} = N_{DOFs}(GFEM) - N_{DOFs}(FEM) \tag{2.35}$$

As mentioned in the previous section, here is a possible explanation for the sudden jump back in the errors when we change h from two to four for $p = 3$ in the GFEM without linear enrichment (*M4*) and SGFEM (*M5*). From Table 2.1, we observe that when we switch h from two to four for $p = 3$, the number of DOFs which is originally larger than that for FEM becomes smaller than that for FEM. This quantitative change may explain the increase in the error. It can be interpreted in this way: when the GFEM-family methods have less DOFs than the FEM, we are loosing some DOFs that help in representing the solution. As a result, the accuracy of the approximation gets lower. We also tried $h = 3$. It shows the increase in error as expected since the number of DOFs is smaller than that for FEM for $h = 3$ and $p = 3$.

2.5.2 Patch test

The patch tests we performed are both based on the coarsest mesh (i.e. $h = 2$). The computed strain energies are shown in Tables 2.5 and 2.6. The results are used to verify which methods can provide the exact solution with the polynomial we cooked up being the exact solution. In other words, the patch tests illustrate the order of accuracy after the PoU is enriched in different manners. The results show that only GFEM gives us the accuracy of the order of enrichment plus one, and other methods give us the accuracy of the same order of enrichment adopted. Recall from Section 2.4, GFEM provides convergence rate of $p + 1$, GFEM without linear enrichment and SGFEM converge at the rate of p. The convergence rate for methods matches the order of accuracy got from these patch tests.

Table 2.1 Number of DOFs for each method

	pBar2		**p=0**	
h	**FEM**	**GFEM**	**GFEM w/o linear**	**SGFEM**
1	2	2	2	2
2	3	3	3	3
3	4	4	4	4
4	5	5	5	5
8	9	9	9	9
16	17	17	17	17
32	33	33	33	33
	pBar4		**p=2**	
h	**FEM**	**GFEM**	**GFEM w/o linear**	**SGFEM**
1	4	6	4	4
2	7	9	6	6
3	10	12	8	8
4	13	15	10	10
8	25	27	18	18
16	49	51	34	34
32	97	99	66	66
	pBar5		**p=3**	
h	**FEM**	**GFEM**	**GFEM w/o linear**	**SGFEM**
1	5	8	6	6
2	9	12	9	9
3	13	16	12	12
4	17	20	15	15
8	33	36	27	27
16	65	68	51	51
32	129	132	99	99
	pBar6		**p=4**	
h	**FEM**	**GFEM**	**GFEM w/o linear**	**SGFEM**
1	6	10	8	8
2	11	15	12	12
3	16	20	16	16
4	21	25	20	20
8	41	45	36	36
16	81	85	68	68
32	161	165	132	132

Table 2.2 First Few Eigenvalues for GFEM (*M3*)
The multiplicity of zero eigenvalues is indicated in bracket unless it is equal to one

h	2	4	8	16	32
	0	0	0	0	0
	1.0000e+00	2.9289e-01	7.6120e-02	1.9215e-02	4.8153e-03
p=0	2.0000e+00	1.0000e+00	2.9289e-01	7.6120e-02	1.9215e-02
		1.7071e+00	6.1732e-01	1.6853e-01	4.3060e-02
		2.0000e+00	1.0000e+00	2.9289e-01	7.6120e-02
	0(2)	0(2)	0(2)	0(2)	0(2)
	1.0000e+00	2.9289e-01	7.6120e-02	1.9215e-02	4.8153e-03
p=1	1.0000e+00	2.9289e-01	7.6120e-02	1.9215e-02	4.8153e-03
	2.0000e+00	1.0000e+00	2.9289e-01	7.6120e-02	1.9215e-02
	2.0000e+00	1.0000e+00	2.9289e-01	7.6120e-02	1.9215e-02
	0(3)	0(3)	0(3)	0(3)	0(3)
	2.7526e-01	5.3752e-02	6.4439e-03	5.1844e-04	3.4889e-05
p=2	7.5000e-01	2.3880e-01	3.6693e-02	3.5575e-03	2.5767e-04
	1.0000e+00	2.9289e-01	7.6120e-02	1.2177e-02	9.5599e-04
	2.0000e+00	5.5730e-01	1.0753e-01	1.9215e-02	2.5053e-03
	0(4)	0(4)	0(4)	0(4)	0(4)
	3.3800e-02	3.8666e-03	2.0935e-04	5.9312e-06	1.1374e-07
p=3	1.0283e-01	2.3244e-02	1.6534e-03	5.7585e-05	1.2333e-06
	1.0000e+00	6.8500e-02	6.6393e-03	2.7585e-04	6.5496e-06
	1.2058e+00	1.0040e-01	1.8029e-02	8.9722e-04	2.3543e-05

Table 2.3 First Few Eigenvalues for GFEM w/o Linear Enrichment (*M4*)
The multiplicity of zero eigenvalues is indicated in bracket unless it is equal to one

h	2	4	8	16	32
	0	0	0	0	0
	1.0000e+00	2.9289e-01	7.6120e-02	1.9215e-02	4.8153e-03
p=0	2.0000e+00	1.0000e+00	2.9289e-01	7.6120e-02	1.9215e-02
		1.7071e+00	6.1732e-01	1.6853e-01	4.3060e-02
		2.0000e+00	1.0000e+00	2.9289e-01	7.6120e-02
	0	0	0	0	0
	7.5000e-01	2.9289e-01	7.6120e-02	1.9215e-02	4.8153e-03
p=2	1.0000e+00	7.5000e-01	2.9289e-01	7.6120e-02	1.9215e-02
	1.0000e+00	8.2322e-01	6.1732e-01	1.6853e-01	4.3060e-02
	1.2500e+00	1.0000e+00	7.5000e-01	2.9289e-01	7.6120e-02
	0	0	0	0	0
	3.1754e-02	4.0443e-02	4.0671e-02	1.9215e-02	4.8153e-03
p=3	4.9854e-02	4.0900e-02	4.0672e-02	4.0672e-02	1.9215e-02
	1.0000e+00	2.9289e-01	7.6120e-02	4.0672e-02	4.0672e-02
	1.0000e+00	8.2496e-01	2.9289e-01	7.6120e-02	4.0672e-02
	0(2)	0	0	0	0
	2.0255e-03	8.6066e-04	1.3500e-03	1.5179e-03	1.5383e-03
p=4	9.1149e-03	1.9443e-03	1.7023e-03	1.5591e-03	1.5388e-03
	1.5039e-01	8.2010e-03	7.6441e-03	7.3184e-03	4.8153e-03
	2.8627e-01	5.0356e-02	1.8732e-02	1.0293e-02	7.1402e-03

Table 2.4 First Few Eigenvalues for SGFEM (*M5*)
The multiplicity of zero eigenvalues is indicated in bracket unless it is equal to one

h	2	4	8	16	32
	0	0	0	0	0
	1.0000e+00	2.9289e-01	7.6120e-02	1.9215e-02	4.8153e-03
p=0	2.0000e+00	1.0000e+00	2.9289e-01	7.6120e-02	1.9215e-02
		1.7071e+00	6.1732e-01	1.6853e-01	4.3060e-02
		2.0000e+00	1.0000e+00	2.9289e-01	7.6120e-02
	0	0	0	0	0
	7.5000e-01	2.9289e-01	7.6120e-02	1.9215e-02	4.8153e-03
p=2	1.0000e+00	7.5000e-01	2.9289e-01	7.6120e-02	1.9215e-02
	1.0000e+00	8.2322e-01	6.1732e-01	1.6853e-01	4.3060e-02
	1.2500e+00	1.0000e+00	7.5000e-01	2.9289e-01	7.6120e-02
	0	0	0	0	0
	9.4634e-03	1.1491e-02	1.1536e-02	1.1536e-02	4.8153e-03
p=3	1.3636e-02	1.1582e-02	1.1536e-02	1.1536e-02	1.1536e-02
	6.8117e-01	2.9289e-01	7.6120e-02	1.9215e-02	1.1536e-02
	8.3282e-01	5.0776e-01	2.9289e-01	7.6120e-02	1.9215e-02
	0(2)	0	0	0	0
	7.3070e-04	3.6585e-04	4.7495e-04	4.8265e-04	4.8269e-04
p=4	3.3035e-03	5.8925e-04	4.9045e-04	4.8273e-04	4.8269e-04
	1.9456e-02	3.2260e-03	3.1818e-03	3.1573e-03	3.1444e-03
	4.2761e-02	6.9120e-03	4.0781e-03	3.3987e-03	3.2128e-03

Table 2.5 Patch Test - Solution Order = 2

Solution: $u(x) = 1 + x + x^2 (order = 2)$ Body Force: $T(x) = -\frac{d^2u}{dx^2} = -2$ BCs: $\frac{du}{dx}(0), \frac{du}{dx}(1)$			
	GFEM	**GFEM w/o linear**	**SGFEM**
p=0	2.1250000000000	2.1250000000000	2.1250000000000
p=1	2.1666666666667	NA	NA
p=2	2.1666666666667	2.1666666666667	2.1666666666667
p=3	2.1666666666667	2.1666666666667	2.1666666666667
exact	2.1666666666667	2.1666666666667	2.1666666666667

Table 2.6 Patch Test - Solution Order = 3

Solution: $u(x) = 1 + x + x^2 + x^3 (order = 3)$ Body Force: $T(x) = -\frac{d^2u}{dx^2} = -(2 + 6x)$ BCs: $\frac{du}{dx}(0), \frac{du}{dx}(1)$			
	GFEM	**GFEM w/o linear**	**SGFEM**
p=0	5.2812500000000	5.2812500000000	5.2812500000000
p=1	5.5651041666667	NA	NA
p=2	5.5666666666667	5.5510416666667	5.5627604166667
p=3	5.5666666666667	5.5666666666667	5.5666666666667
p=4	5.5666666666667	5.5666666666667	5.5666666666667
exact	5.5666666666667	5.5666666666667	5.5666666666667

2.6 Modifications on SGFEM

This section presents some modified methods based on the standard SGFEM. The idea to construct these discretization methods comes from the features for *M1-M5* we observe from previous sections.

2.6.1 Modified SGFEM with linear enrichment not subtracting FE interpolant: SGFEM Mod1

Since we find that for GFEM $p = 0$ and $p = 1$ yield the same conditioning from Section 2.4.1 and SGFEM yields better accuracy from Section 2.4.3, we here construct a modified version of SGFEM with linear enrichment not subtracting FE interpolant (*M6*) as described in Section 2.2. The results for this method are shown in Figures 2.10 and 2.11. This method yields the following results:

- It gives the same accuracy as the standard GFEM (*M3*) does, which means it is of higher accuracy than standard SGFEM (*M5*), and of the same level accuracy as p-Lagrange and p-Hierarchical FEM. The convergence rate for *M6* is equal to the enrichment order plus one (i.e., $\beta = p+1$).
- Its conditioning behaves in the same way as the standard GFEM, rather than in the way of the standard SGFEM. This may be due to the linear enrichment itself. Recall that for GFEM, when the linear enrichment is skipped, the conditioning gets stable accordingly. So, it indicates that it is the linear enrichment that causes the bad conditioning.
- For low p-order, scaled condition numbers (SCNs) for *M6* are identical to those in the standard GFEM. For high p-order, its SCNs are a bit higher than those in the GFEM.
- The number of zero eigenvalues is the same as that in the standard GFEM which is equal to the order of enrichment plus one (e.g. for p=2, we have three zero eigenvalues for all meshes).

Therefore, SGFEM Mod1 holds high accuracy but not good conditioning as compared to the standard SGFEM from the discussion above. At this point, the linear enrichment seems to be the key component that causes the different behaviors in the accuracy and conditioning between the GFEM and the SGFEM. However, this opinion is not conclusive. In the next section, further remarks will be stated based on the results for *M7*.

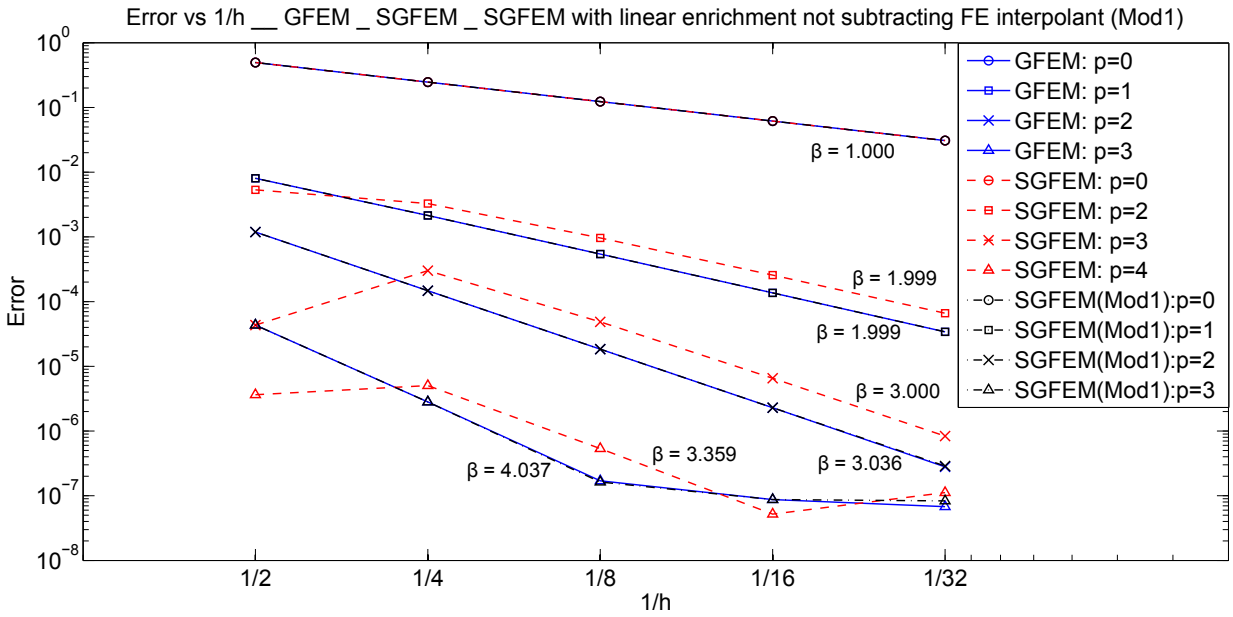


Fig. 2.10 Relative error in energy norm with respect to element size for GFEM (*M3*), SGFEM (*M5*), and SGFEM Mod1 (*M6*)

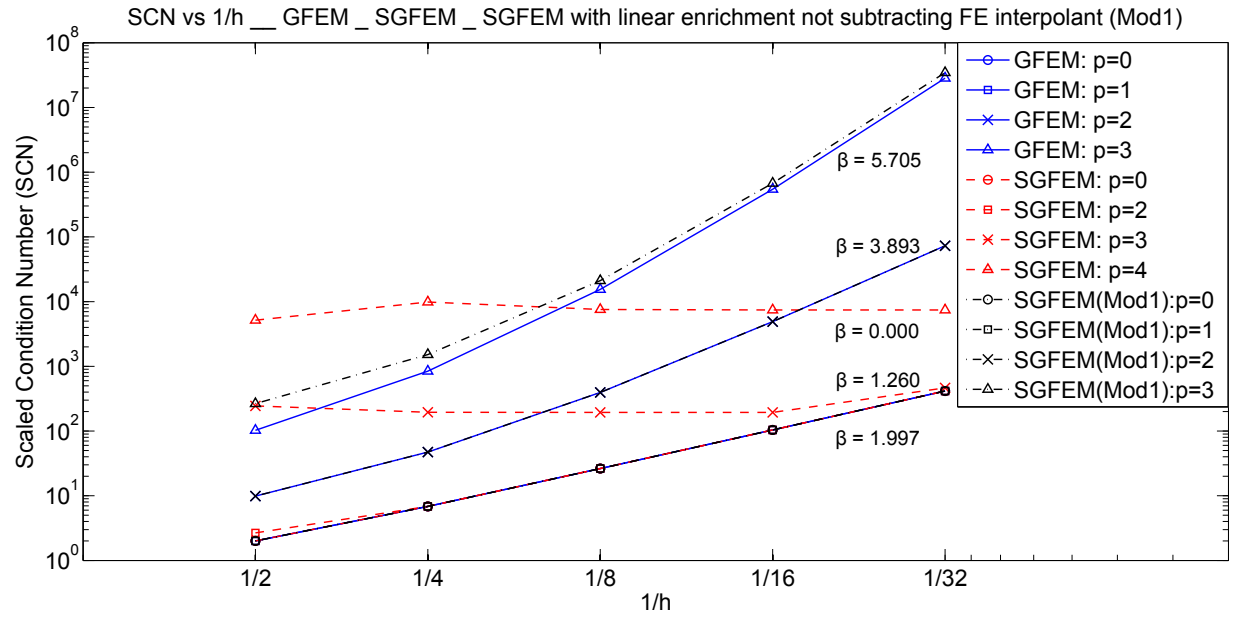


Fig. 2.11 SCN with respect to element size for GFEM (*M3*), SGFEM (*M5*), and SGFEM Mod1 (*M6*)

Table 2.7 First Few Eigenvalues for SGFEM Mod1 (*M6*)
The multiplicity of zero eigenvalues is indicated in bracket unless it is equal to one

h	2	4	8	16	32
	0	0	0	0	0
	1.0000e+00	2.9289e-01	7.6120e-02	1.9215e-02	4.8153e-03
p=0	2.0000e+00	1.0000e+00	2.9289e-01	7.6120e-02	1.9215e-02
		1.7071e+00	6.1732e-01	1.6853e-01	4.3060e-02
		2.0000e+00	1.0000e+00	2.9289e-01	7.6120e-02
	0(2)	0(2)	0(2)	0(2)	0(2)
	1.0000e+00	2.9289e-01	7.6120e-02	1.9215e-02	4.8153e-03
p=1	1.0000e+00	2.9289e-01	7.6120e-02	1.9215e-02	4.8153e-03
	2.0000e+00	1.0000e+00	2.9289e-01	7.6120e-02	1.9215e-02
	2.0000e+00	1.0000e+00	2.9289e-01	7.6120e-02	1.9215e-02
	0(3)	0(3)	0(3)	0(3)	0(3)
	2.7526e-01	5.3752e-02	6.4439e-03	5.1844e-04	3.4889e-05
p=2	7.5000e-01	2.3880e-01	3.6693e-02	3.5575e-03	2.5767e-04
	1.0000e+00	2.9289e-01	7.6120e-02	1.2177e-02	9.5599e-04
	2.0000e+00	5.5730e-01	1.0753e-01	1.9215e-02	2.5053e-03
	0(4)	0(4)	0(4)	0(4)	0(4)
	1.5861e-02	2.6014e-03	1.8506e-04	5.7665e-06	1.1300e-07
p=3	3.1653e-02	1.0940e-02	1.1956e-03	5.2594e-05	1.2061e-06
	7.6382e-01	2.4744e-02	3.9538e-03	2.3232e-04	6.2636e-06
	8.9985e-01	3.0930e-02	8.9674e-03	6.8744e-04	2.1873e-05

2.6.2 Modified SGFEM with linear enrichment not subtracting FE interpolant and no quadratic enrichment: SGFEM Mod2

Based on the observation from SGFEM Mod1 (*M6*), we come up with SGFEM Mod2 (*M7*) by skipping the quadratic enrichment since for SGFEM Mod1 and $p = 1$ the convergence is already quadratic ($\beta = p + 1 = 2$). Therefore, we do not need $p = 2$ enrichment which provides the quadratic convergence in the standard SGFEM and jump to $p = 3$. The shape functions for SGFEM Mod2 are as described in Section 2.2. The results of error and SCN are shown in Figures 2.12 and 2.13. The SGFEM Mod2 yields the following results:

- It gives a bit lower accuracy than the standard SGFEM (*M5*) does, which means it is less accurate than the standard GFEM (*M3*), and of lower accuracy than *p*-Lagrange (*M1*) and *p*-Hierarchical FEM (*M2*).
- For cubic enrichment, it shows a convergence rate of order three; for quartic enrichment it shows a convergence rate of order four. This means for $p \leq 1$ the rate of convergence is equal to $p+1$, and for $p \geq 3$ the rate of convergence is equal to the enrichment order p.
- Its conditioning behaves similarly to the standard SGFEM. SCNs are nearly constant as we refine the mesh. For finer meshes, it shows a growth in the SCN of order h^{-2}. Additionally, its SCNs are even smaller than those of the standard SGFEM except for the finest meshes.
- The number of zero eigenvalues is one for $p = 0$, and two for all other cases upto quartic enrichment. This observation does not match the expression we achieve in Section 2.5.1. This issue will not be addressed in this thesis. One possible explanation is that the linear enrichment introduce one additional spurious zero eigenvalue to the system.

Therefore, SGFEM Mod2 shows similar curves to the standard SGFEM from the discussion above. It holds good conditioning but lower accuracy. Combining this observation with the behaviors of SGFEM Mod1 (*M6*) and GFEM without linear enrichment (*M4*), it is the completeness of the enrichment polynomials that denotes the different behaviors of the GFEM and the SGFEM. Thus, we can conclude that if the set of polynomials used for enrichment is complete, the method will yield GFEM-type behavior: higher accuracy and bad conditioning; if the enrichment polynomials are not complete, the method will yield SGFEM-type behavior: a bit lower accuracy and better conditioning.

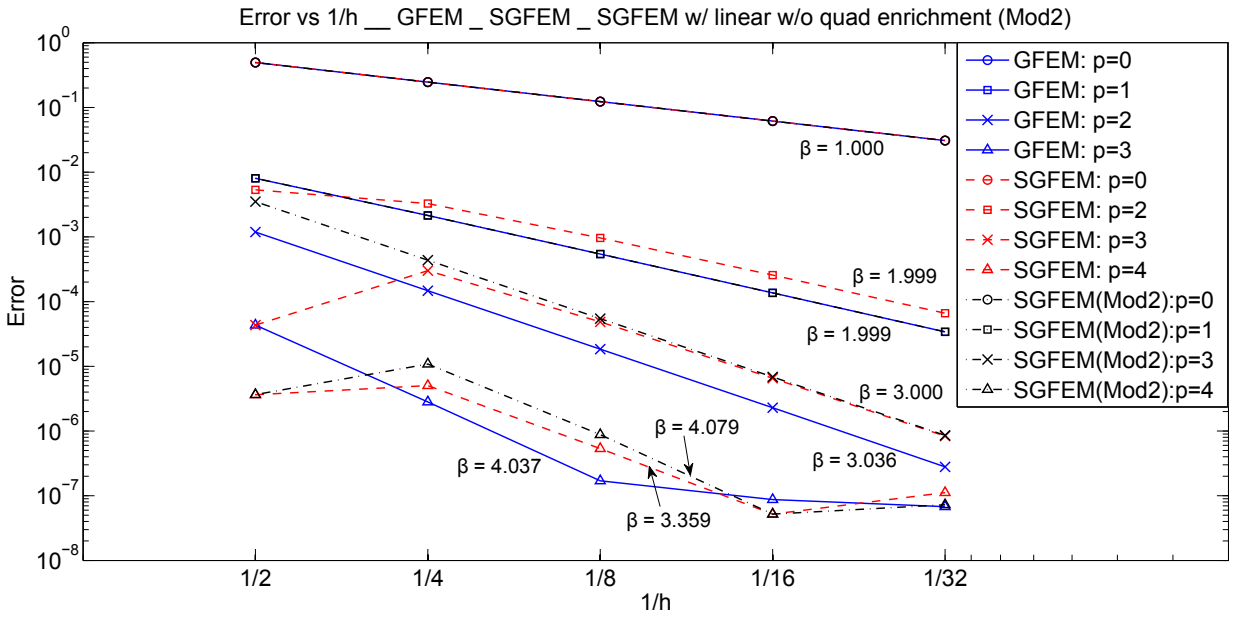


Fig. 2.12 Relative error in energy norm with respect to element size for GFEM (*M3*), SGFEM (*M5*), and SGFEM Mod2 (*M7*)

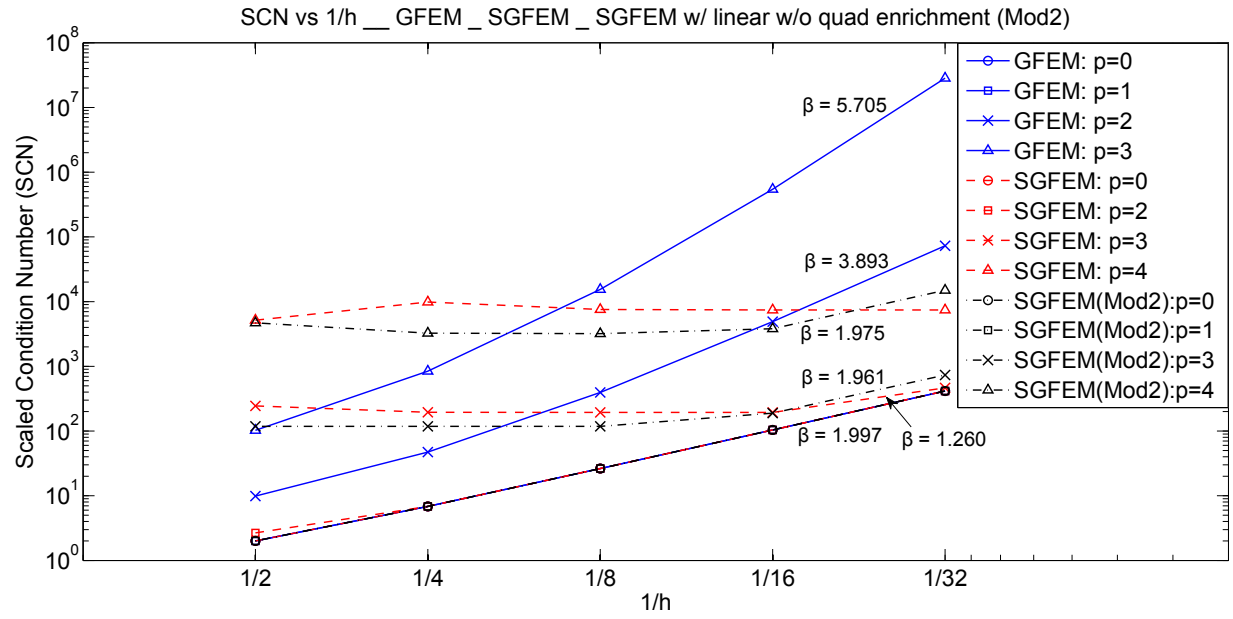


Fig. 2.13 SCN with respect to element size for GFEM (*M3*), SGFEM (*M5*), and SGFEM Mod2 (*M7*)

Table 2.8 First Few Eigenvalues for SGFEM Mod2 (*M7*)
The multiplicity of zero eigenvalues is indicated in bracket unless it is equal to one

h	2	4	8	16	32
	0	0	0	0	0
	1.0000e+00	2.9289e-01	7.6120e-02	1.9215e-02	4.8153e-03
p=0	2.0000e+00	1.0000e+00	2.9289e-01	7.6120e-02	1.9215e-02
		1.7071e+00	6.1732e-01	1.6853e-01	4.3060e-02
		2.0000e+00	1.0000e+00	2.9289e-01	7.6120e-02
	0(2)	0(2)	0(2)	0(2)	0(2)
	1.0000e+00	2.9289e-01	7.6120e-02	1.9215e-02	4.8153e-03
p=1	1.0000e+00	2.9289e-01	7.6120e-02	1.9215e-02	4.8153e-03
	2.0000e+00	1.0000e+00	2.9289e-01	7.6120e-02	1.9215e-02
	2.0000e+00	1.0000e+00	2.9289e-01	7.6120e-02	1.9215e-02
	0(2)	0(2)	0(2)	0(2)	0(2)
	2.9697e-02	2.9697e-02	2.9697e-02	1.8601e-02	4.7772e-03
p=3	1.3649e-01	6.2786e-02	3.8370e-02	1.9215e-02	4.8153e-03
	4.5652e-01	1.3649e-01	6.2786e-02	2.9697e-02	1.8601e-02
	1.0000e+00	1.5427e-01	6.6114e-02	3.1890e-02	1.9215e-02
	0(2)	0(2)	0(2)	0(2)	0(2)
	9.3349e-04	1.2697e-03	1.2825e-03	1.0723e-03	2.7275e-04
p=4	1.6446e-03	1.2997e-03	1.2847e-03	1.2836e-03	1.0749e-03
	3.6787e-02	1.3844e-02	4.1203e-03	1.2912e-03	1.2834e-03
	4.3994e-02	2.9481e-02	1.3730e-02	4.1117e-03	1.2874e-03

2.6.3 Modified SGFEM without shifting or scaling: SGFEM Mod3

In this section and the following one, a different type of modifications to SGFEM is established. Instead of skipping enrichment terms as in *M6* and *M7*, we focus on the behavior of the methods if scaling or shifting is absent in the enrichment. The enrichment terms hold the same order as standard SGFEM, but they are formulated without shifting or scaling (Section 2.6.3) and only without scaling (Section 2.6.4).

From Figures 2.14 and 2.15, SGFEM without shifting or scaling yields (*M8*) almost the same level of accuracy and convergence rates as SGFEM does. However, the Scaled Condition Numbers are much worse for high p-order. Not only are the values of SCNs much larger, but also it shows a growth in SCNs of high rates (i.e. h^{-2} for $p = 3$, h^{-4} for $p = 4$). The numbers of zero eigenvalues shown in Table 2.9 are the same as those for standard SGFEM (*M5*), which means that shifting or scaling are not affecting the number of resulting spurious modes.

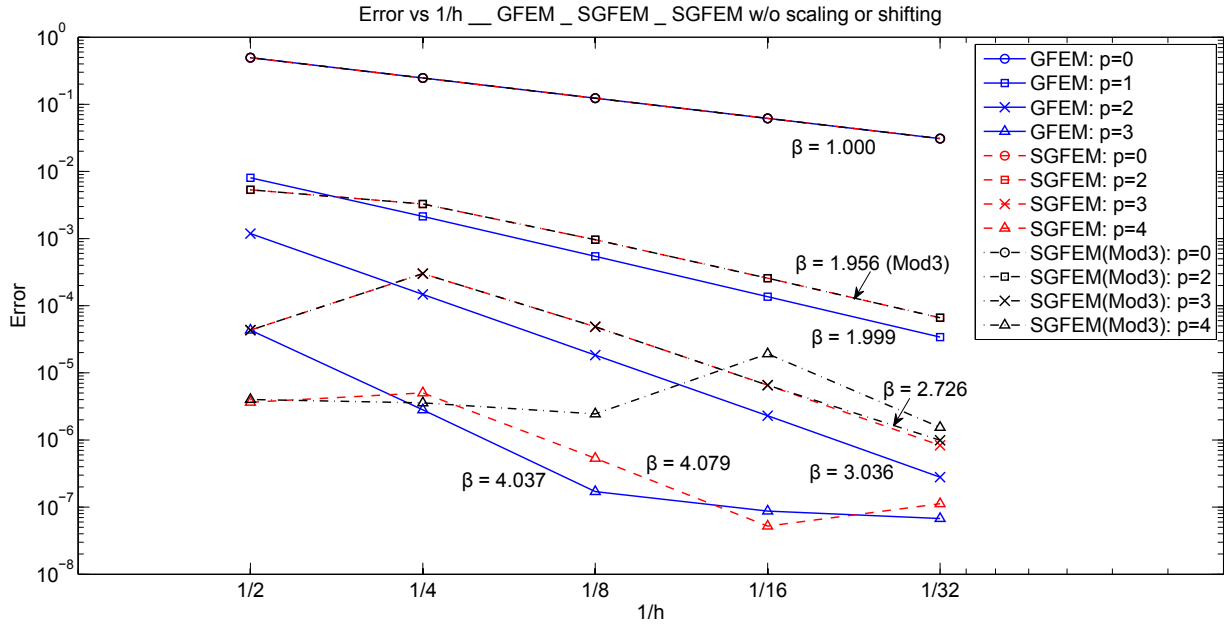


Fig. 2.14 Relative error in energy norm with respect to element size for GFEM (*M3*), SGFEM (*M5*), and SGFEM Mod3 (*M8*)

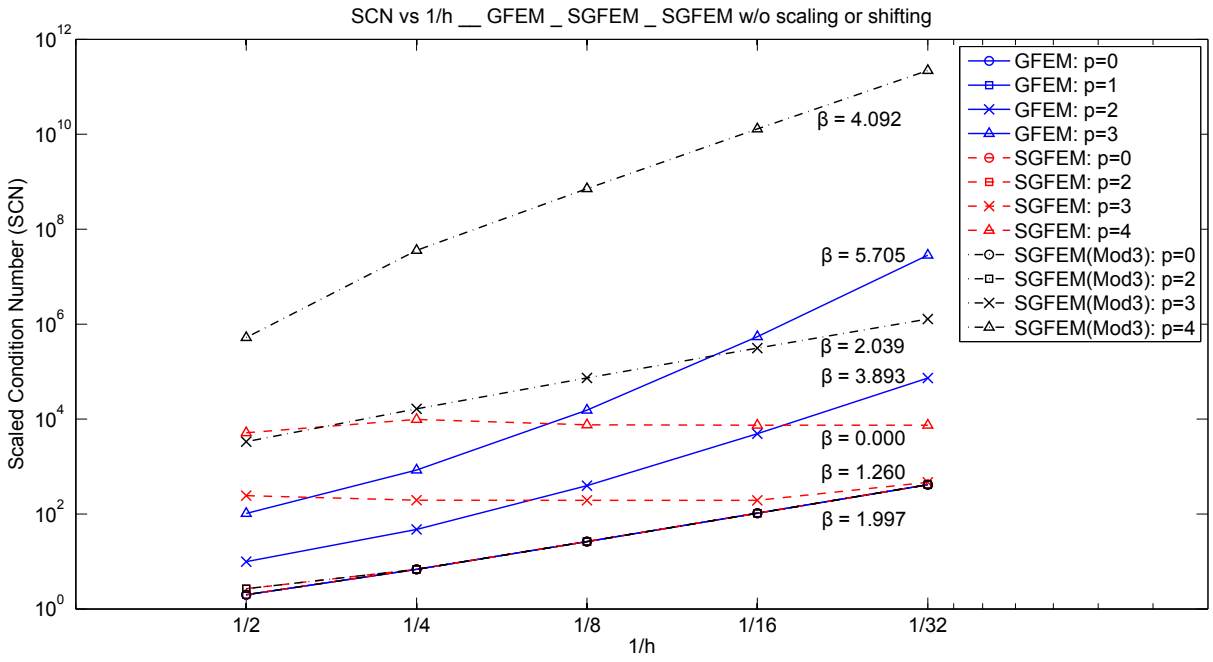


Fig. 2.15 SCN with respect to element size for GFEM (*M3*), SGFEM (*M5*), and SGFEM Mod3 (*M8*)

Table 2.9 First Few Eigenvalues for SGFEM Mod3 (*M8*)
The multiplicity of zero eigenvalues is indicated in bracket unless it is equal to one

h	2	4	8	16	32
	0	0	0	0	0
	1.0000e+00	2.9289e-01	7.6120e-02	1.9215e-02	4.8153e-03
p=0	2.0000e+00	1.0000e+00	2.9289e-01	7.6120e-02	1.9215e-02
		1.7071e+00	6.1732e-01	1.6853e-01	4.3060e-02
		2.0000e+00	1.0000e+00	2.9289e-01	7.6120e-02
	0	0	0	0	0
	7.5000e-01	2.9289e-01	7.6120e-02	1.9215e-02	4.8153e-03
p=2	1.0000e+00	7.5000e-01	2.9289e-01	7.6120e-02	1.9215e-02
	1.0000e+00	8.2322e-01	6.1732e-01	1.6853e-01	4.3060e-02
	1.2500e+00	1.0000e+00	7.5000e-01	2.9289e-01	7.6120e-02
	0	0	0	0	0
	7.4106e-04	1.5148e-04	3.3834e-05	8.0109e-06	1.9499e-06
p=3	1.0044e-02	7.5914e-03	1.2735e-03	2.4760e-04	5.2891e-05
	7.6908e-02	9.7919e-03	2.0913e-03	3.3825e-04	6.4309e-05
	1.0000e+00	1.9897e-02	3.1792e-03	4.3622e-04	7.5577e-05
	0(2)	0	0	0	0
	7.0539e-06	1.0345e-07	5.2398e-09	2.9013e-10	1.7021e-11
p=4	7.1460e-04	7.2523e-07	2.5655e-08	1.0708e-09	5.3127e-11
	2.8754e-03	1.0969e-05	1.4626e-07	3.3154e-09	1.0897e-10
	2.2910e-02	1.3277e-04	4.0383e-07	6.6810e-09	1.7443e-10

2.6.4 Modified SGFEM without scaling: SGFEM Mod4

From Figures 2.16 and 2.17, SGFEM without scaling (*M9*) yields almost the same errors and convergence rates as standard SGFEM does. An exception is the case of fine meshes and enrichments of degree $p = 4$. From Table 2.10 and Figure 2.17, the number of zero eigenvalues, first few eigenvalues, SCNs, and growth rates in SCNs are identical in both methods. Considering the overall behavior of *M5* and *M9*, the scaling of polynomial enrichments is recommended.

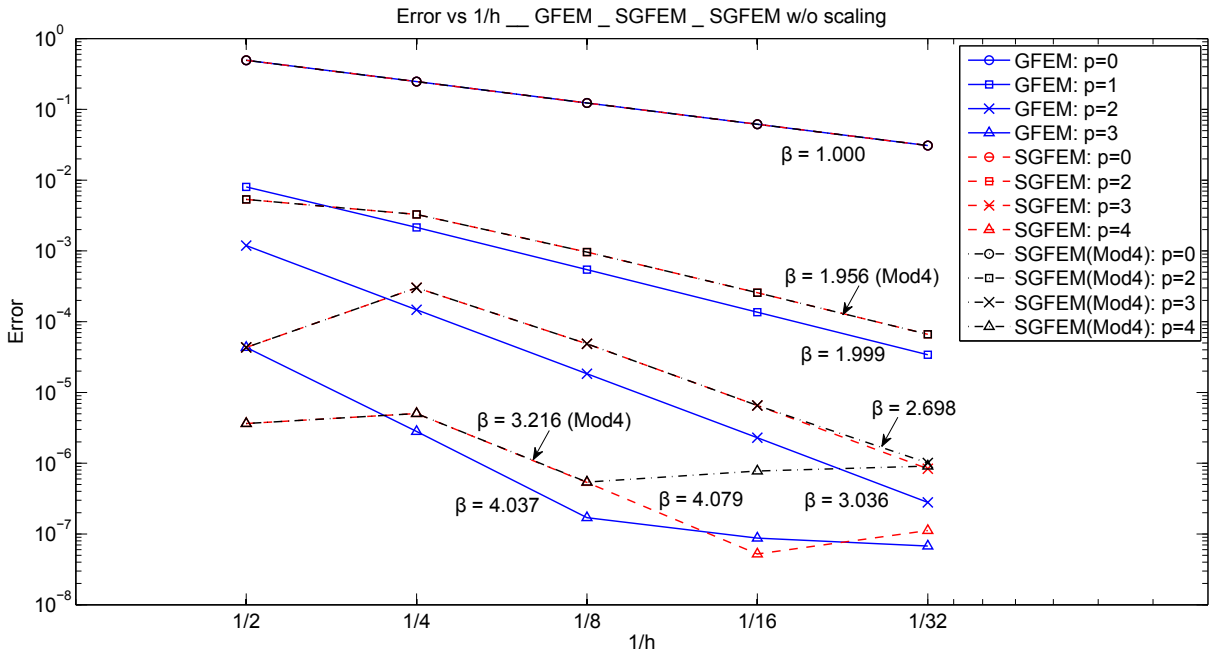


Fig. 2.16 Relative error in energy norm with respect to element size for GFEM (*M3*), SGFEM (*M5*), and SGFEM Mod4 (*M9*)

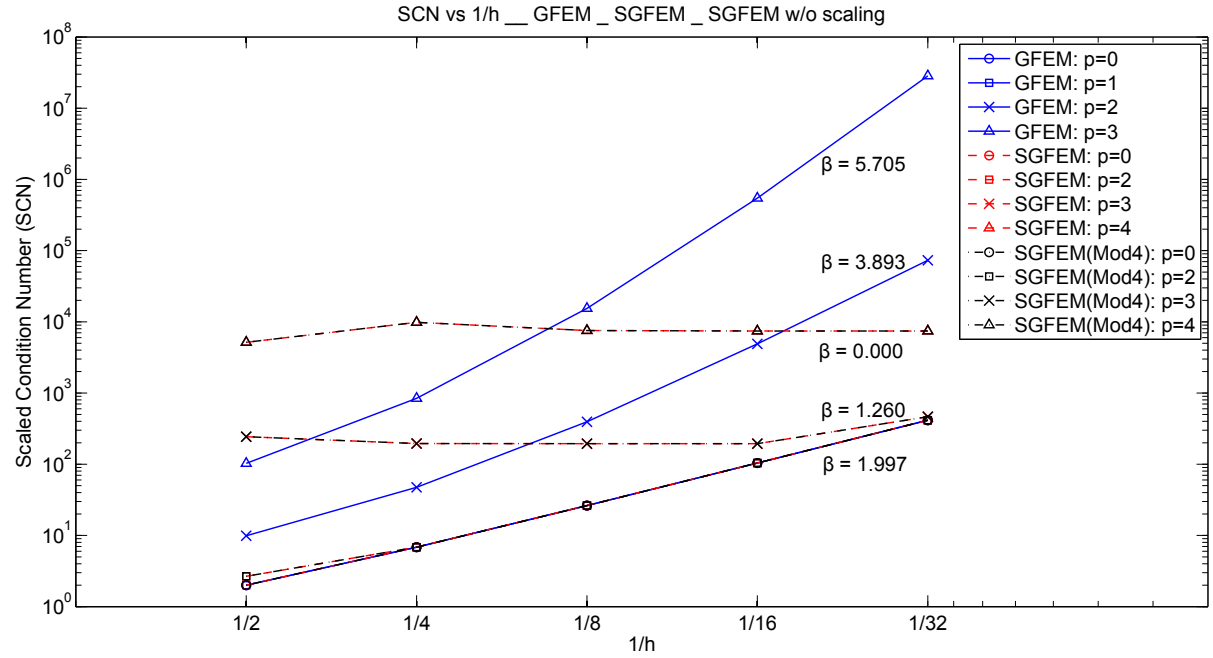


Fig. 2.17 SCN with respect to element size for GFEM (*M3*), SGFEM (*M5*), and SGFEM Mod4 (*M9*)

Table 2.10 First Few Eigenvalues for SGFEM Mod4 (*M9*)
The multiplicity of zero eigenvalues is indicated in bracket unless it is equal to one

h	2	4	8	16	32
	0	0	0	0	0
	1.0000e+00	2.9289e-01	7.6120e-02	1.9215e-02	4.8153e-03
p=0	2.0000e+00	1.0000e+00	2.9289e-01	7.6120e-02	1.9215e-02
		1.7071e+00	6.1732e-01	1.6853e-01	4.3060e-02
		2.0000e+00	1.0000e+00	2.9289e-01	7.6120e-02
	0	0	0	0	0
	7.5000e-01	2.9289e-01	7.6120e-02	1.9215e-02	4.8153e-03
p=2	1.0000e+00	7.5000e-01	2.9289e-01	7.6120e-02	1.9215e-02
	1.0000e+00	8.2322e-01	6.1732e-01	1.6853e-01	4.3060e-02
	1.2500e+00	1.0000e+00	7.5000e-01	2.9289e-01	7.6120e-02
	0	0	0	0	0
	9.4634e-03	1.1491e-02	1.1536e-02	1.1536e-02	4.8153e-03
p=3	1.3636e-02	1.1582e-02	1.1536e-02	1.1536e-02	1.1536e-02
	6.8117e-01	2.9289e-01	7.6120e-02	1.9215e-02	1.1536e-02
	8.3282e-01	5.0776e-01	2.9289e-01	7.6120e-02	1.9215e-02
	0(2)	0	0	0	0
	7.3070e-04	3.6585e-04	4.7495e-04	4.8265e-04	4.8269e-04
p=4	3.3035e-03	5.8925e-04	4.9045e-04	4.8273e-04	4.8269e-04
	1.9456e-02	3.2260e-03	3.1818e-03	3.1573e-03	3.1444e-03
	4.2761e-02	6.9120e-03	4.0781e-03	3.3987e-03	3.2128e-03

2.7 Summary for 1-D Numerical Experiments

Considering all methods for one-dimensional BVP discussed in this study, we may draw the following conclusions about high-order GFEM and SGFEM approximations:

1. GFEM with complete enrichment and SGFEM Mod1 are the only two methods that provide convergence rates in the energy norm equal to $p+1$. All other methods, namely GFEM without linear enrichment, SGFEM, and SGFEM Mod2, provide convergence rates equal to the polynomial order of the enrichments. At this point, the following clarification needs to be made. Before skipping the quadratic term SGFEM Mod2 yields $p+1$ convergence. However, that formulation is actually the same as standard GFEM formulation. Thus, strictly speaking, SGFEM Mod2 is providing the rate of convergence equal to p.

2. GFEM is accurate but its conditioning quickly deteriorates for cubic and higher-order approximations ($p \geq 2$) , while GFEM without linear enrichment, SGFEM, and SGFEM Mod2 are less accurate but yield much better and stable conditioning for high p-order.

3. SGFEM Mod3 can provide the same accuracy as standard SGFEM for low order of p. But the conditioning of SGFEM Mod3 is much worse as p-order increases.

4. SGFEM Mod4 behaves the same way in both accuracy and conditioning as standard SGFEM does except for the finer meshes of the highest p-order. Therefore, generally the scaling to the enrichment is recommended in similar cases.

5. GFEM with complete enrichment is the most effective method for quadratic approximations (i.e., with linear enrichment, $p = 1$). SGFEM or SGFEM Mod2 are recommended for approximations of degree three or higher ($p \geq 2$).

6. Scaling and shifting are not affecting the LD of the resulting system. Skipping the linear enrichment (*M4*, *M5*, and *M8*) can fix the LD issue as well as improve the conditioning of the matrix. Skipping the quadratic enrichment (*M7*) can also provide good conditioning and get rid of some spurious zero eigenvalues, but still leaves one more zero eigenvalue as compared to the methods dropping linear term. The completeness of the enrichment polynomials decides whether a method behaves like GFEM or SGFEM as discussed in Section 2.6.

7. By comparing *M8* and *M9*, shifting of the enrichment is necessary to achieve good conditioning. Although the linear term is skipped in *M8*, its conditioning is not as stable as that for the standard SGFEM. Thus shifting of the enrichment is always recommended.

CHAPTER 3

TWO-DIMENSIONAL NUMERICAL EXPERIMENT

In this chapter, a study of selected discretization methods based on a two-dimensional BVP is performed. The objective of this investigation on a 2-D problem is to verify our conclusions drawn from the 1-D problem.

For the two-dimensional problem, the system of equations are solved using Babuška algorithm described in Section 2.3. Eigenvalues and SCNs are computed through the same approach as in the 1-D problem. The cut-off values for non-zero eigenvalues is 10^{-13} as well.

3.1 Two-dimensional Model Problem

The two-dimensional numerical experiments are based on the Neumann Boundary Value Problem (BVP) defined as follow.

Governing Equations

$$-\mathbf{B}^T \boldsymbol{\sigma} = \mathbf{T}(x,y) \qquad x \in [0,\,1],\;\; y \in [0,\,1] \tag{3.1}$$

where

$$\mathbf{B} = \begin{bmatrix} \frac{\partial}{\partial x} & 0 \\ 0 & \frac{\partial}{\partial y} \\ \frac{\partial}{\partial y} & \frac{\partial}{\partial x} \end{bmatrix} \tag{3.2}$$

Strain-displacement relations

$$\boldsymbol{\varepsilon} = \mathbf{B}\,\mathbf{u} \tag{3.3}$$

Stress-strain relation is denoted by the Plane Strain state which reads

$$\sigma = \mathbf{D}\varepsilon \tag{3.4}$$

where

$$\mathbf{D} = \frac{E}{(1+\nu)(1-2\nu)} \begin{bmatrix} 1-\nu & \nu & 0 \\ \nu & 1-\nu & 0 \\ 0 & 0 & \frac{1-2\nu}{2} \end{bmatrix} \tag{3.5}$$

The Neumann BCs (edge tractions) applied to the problem domain are given by

$$\sigma\, \mathbf{n} = \bar{\mathbf{f}} \quad on\ \Gamma \tag{3.6}$$

where Γ denotes the boundary of the square domain and $\bar{\mathbf{f}}$ is the prescribed traction computed using the manufactured solution given by (3.7).

The manufactured solution of the BVP is taken as

$$\mathbf{u} = \begin{bmatrix} u_x \\ u_y \end{bmatrix} = \begin{bmatrix} \sin \pi x\ \sin \pi y \\ \sin \pi x\ \sin \pi y \end{bmatrix} \tag{3.7}$$

The manufactured solution is a smooth function as plotted in Figure 3.1. Material properties are set as

$$E = 1.0,\ \ \nu = 0.30,\ \ t = 1.0 \tag{3.8}$$

where E is the elastic modulus, ν is the Poisson's ratio, and t is the domain thickness.

The exact strain energy is given by

$$U_{exact} = \frac{1}{2} t \int_0^1 \int_0^1 (\mathbf{Bu})^T \mathbf{D} (\mathbf{Bu})\, dxdy = 4.270501904317514 \tag{3.9}$$

3.2 Discretization Methods for 2-D

M1. Lagrange FEM:

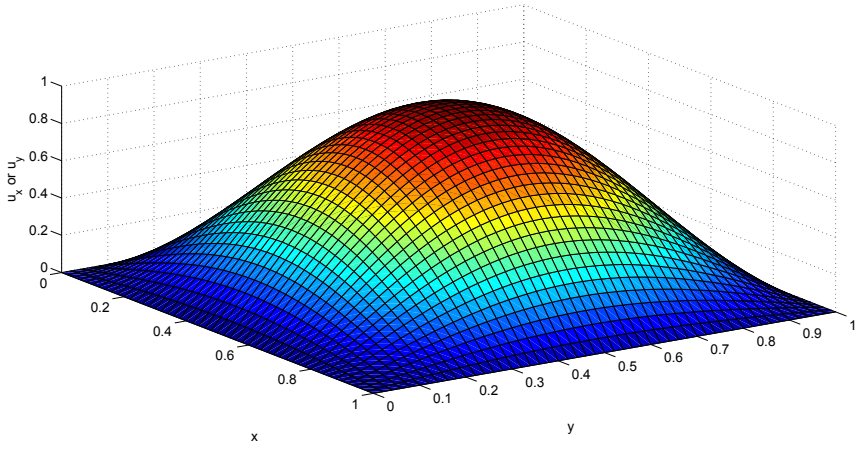


Fig. 3.1 Manufactured solution for two-dimensional problem

The Lagrange FEM is the discretization method using TRIA3 and TRIA6 elements.

M2. Standard GFEM:

In two-dimensional case, the same set of enrichment is adopted in both x and y direction for all the following methods. The enrichments for the standard GFEM come from Pascal triangle of monomials. The resulting approximation basis in each direction (i.e., x and y) for the standard GFEM in 2-D is then given by

$$\phi_\alpha = \varphi_\alpha \times \{\underbrace{1}_{\text{p=0}}, \underbrace{\hat{x}, \hat{y}}_{\text{p=1}}, \underbrace{\hat{x}^2, \hat{x}\hat{y}, \hat{y}^2}_{\text{p=2}}, \underbrace{\hat{x}^3, \hat{x}^2\hat{y}, \hat{x}\hat{y}^2, \hat{y}^3}_{\text{p=3}}, ...\} \tag{3.10}$$

where $\hat{x}$ and $\hat{y}$ are the scaled and shifted coordinates for enrichments which read

$$\hat{x} = \frac{x - x_\alpha}{h_{\alpha x}}, \quad \hat{y} = \frac{y - y_\alpha}{h_{\alpha y}} \tag{3.11}$$

and φ_α is the linear PoU function (i.e., the shape function for TRIA3 element) in x or y direction at node α (i.e., the linear Lagrange shape function) and ϕ_α is the GFEM shape function in x or y direction at node α after enrichment. Formulations for the following discretization methods share the same notations of φ_α, ϕ_α, $\hat{x}$ and $\hat{y}$.

The standard GFEM is also denoted as GFEM with $pou = 0$ in the labels of the plots and the discussion in the following section.

M3. GFEM without linear enrichments:

The enrichments for the GFEM without linear enrichments come from Pascal triangle of monomials except that the linear terms are skipped. The resulting approximation basis in

each direction (i.e., x and y) for GFEM without linear enrichments in 2-D are given by

$$\phi_\alpha = \varphi_\alpha \times \{\underbrace{1}_{\text{p=0}}, \underbrace{\hat{x}^2, \hat{x}\hat{y}, \hat{y}^2}_{\text{p=2}}, \underbrace{\hat{x}^3, \hat{x}^2\hat{y}, \hat{x}\hat{y}^2, \hat{y}^3}_{\text{p=3}}, ...\} \tag{3.12}$$

GFEM without linear enrichments is also denoted as GFEM with $pou = 1$ in the labels of the plots and the discussion in the following section.

M4. Standard SGFEM:

Because of the subtraction of the FE interpolant, the linear enrichment is always skipped for the standard SGFEM. Therefore, it is also denoted as SGFEM with $pou = 1$ in the labels of the plots and the discussion in the following section. The enrichments for the standard SGFEM come from Pascal triangle of monomials except that the linear terms are skipped and the piecewise linear FE interpolants $\mathcal{I}_{\omega_\alpha}$ are subtracted from each term. The resulting approximation basis in each direction (i.e., x and y) for the standard SGFEM in 2-D are given by

$$\begin{aligned}\phi_\alpha = \varphi_\alpha \times \{&\underbrace{1}_{\text{p=0}}, \underbrace{\hat{x}^2 - \mathcal{I}_{\omega_\alpha}(\hat{x}^2), \hat{x}\hat{y} - \mathcal{I}_{\omega_\alpha}(\hat{x}\hat{y}), \hat{y}^2 - \mathcal{I}_{\omega_\alpha}(\hat{y}^2)}_{\text{p=2}}, \\ &\underbrace{\hat{x}^3 - \mathcal{I}_{\omega_\alpha}(\hat{x}^3), \hat{x}^2\hat{y} - \mathcal{I}_{\omega_\alpha}(\hat{x}^2\hat{y}), \hat{x}\hat{y}^2 - \mathcal{I}_{\omega_\alpha}(\hat{x}\hat{y}^2), \hat{y}^3 - \mathcal{I}_{\omega_\alpha}(\hat{y}^3)}_{\text{p=3}}, ...\}\end{aligned} \tag{3.13}$$

3.3 2-D Numerical Experiments Results

In this section, a brief discussion on the results of the 2-D numerical experiment is made by comparing the accuracy and conditioning between each method. The relative error in energy norm and the scaled condition number are the two quantities adopted to measure the quality of the approximation. They are computed in the same way as described in Sections 2.3 and 2.4.

Since in 2-D problems the number of DOFs for methods with $pou = 1$ and higher p-order can be less than that for methods with $pou = 0$ and lower p-order, comparisons of quantities with respect to element size may be unfair to some extent. In addition to plots with the element size in the x-axis, the number of total DOFs is also used in plotting curves. Figures 3.2 and 3.3 are plotted with element size in the x-axis and Figures 3.5 and 3.6 are plotted with number of DOFs in the x-axis. For a better resolution of Figure 3.3, Figure 3.4 shows only those curves with low approximation orders.

The resulting behaviors for 2-D problem are basically the same as what we learnt from 1-D problem in the previous chapter.

From plots with element size being x-axis (Figures 3.2, 3.3, and 3.4), we observe that GFEM with complete enrichment (*M2*) is the only method with its convergence rate equal to $p+1$. And the convergence rate for all other methods is equal to p. As for accuracy, the standard GFEM and Lagrange FEM are of the highest accuracy. With $pou = 1$, SGFEM (*M4*) gives lower error than GFEM without linear enrichments (*M3*), while *M4* yields slightly higher values of SCNs than *M3*. For standard GFEM, it shows a growth in SCNs of h^{-2} for $p = 0$ and 1, h^{-4} for $p = 2$, and h^{-12} for $p = 3$. The standard SGFEM and GFEM without linear enrichments both give stable values of SCNs for coarse meshes and show a growth in SCNs of h^{-2} for $p = 0$, 2, and 3 when we refine the mesh. For $p = 4$, both *M4* and *M3* give us stabilized flat curves for SCNs throughout all meshes. For $p = 2$, the values of SCNs for SGFEM and GFEM without linear enrichment are always smaller than FEM TRIA6. And for the finest meshes, SGFEM and GFEM without linear enrichments provide smaller SCNs than FEM TRIA6 even for $p = 3$.

From plots with number of DOFs being x-axis (Figures 3.5 and 3.6), we observe that though standard GFEM yields worse SCNs, it can use the least number of DOFs to reach the same level of accuracy as compared to the other methods with the same convergence rate. For coarse meshes, the standard GFEM with $p = 1$ is even more accurate than GFEM without linear enrichments and $p = 3$. And the same observation works for standard GFEM with $p = 2$ and GFEM without linear enrichments and $p = 4$. As for SCNs, GFEM without linear enrichments and standard SGFEM yield smaller SCN values than the other two methods for a given number of DOFs.

Figure 3.7 shows the plot of errors in energy norm with respect to the corresponding SCNs. It may provide the reader with a different view to understand the methods. We observe that for low p-order the standard GFEM gives smaller error for a certain value of SCN while for high order approximation the standard SGFEM and GFEM without linear enrichments behave much better.

In Tables 3.1, 3.2, 3.3, and 3.4, the first few smallest nonzero eigenvalues, the largest eigenvalues, and the multiplicity of zero eigenvalues are tabulated for each method. The expression for the number of spurious zero eigenvalues for 1-D problem is not working in 2-D case. Simply counting the difference between DOFs is not applicable because the two dimensions are couple in the PoU basis and the enrichment functions. Except the standard GFEM, all other methods eliminate spurious modes and preserve only three zero eigenvalues representing rigid body motion in 2-D. Thus, the LD issue is fixed by skipping the linear enrichment, which is the same as in 1-D case.

By observing the first few smallest nonzero eigenvalues and the largest one, the stabilization of the conditioning can also be identified for GFEM without linear enrichments and standard SGFEM.

The order of magnitude of their smallest nonzero eigenvalues do not decrease rapidly as the mesh is refined. And the largest eigenvalues also remain at the same level of magnitude for a certain p-order.

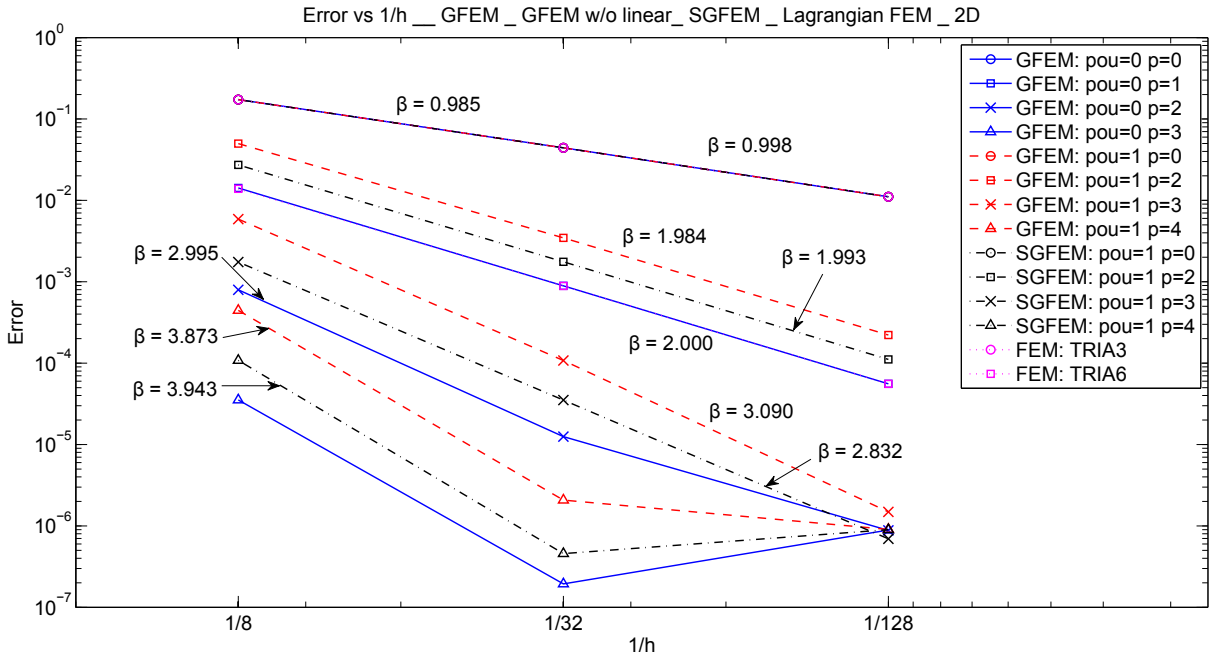


Fig. 3.2 Relative error in energy norm with respect to element size for GFEM, GFEM without linear enrichments, SGFEM, and FEM in 2D

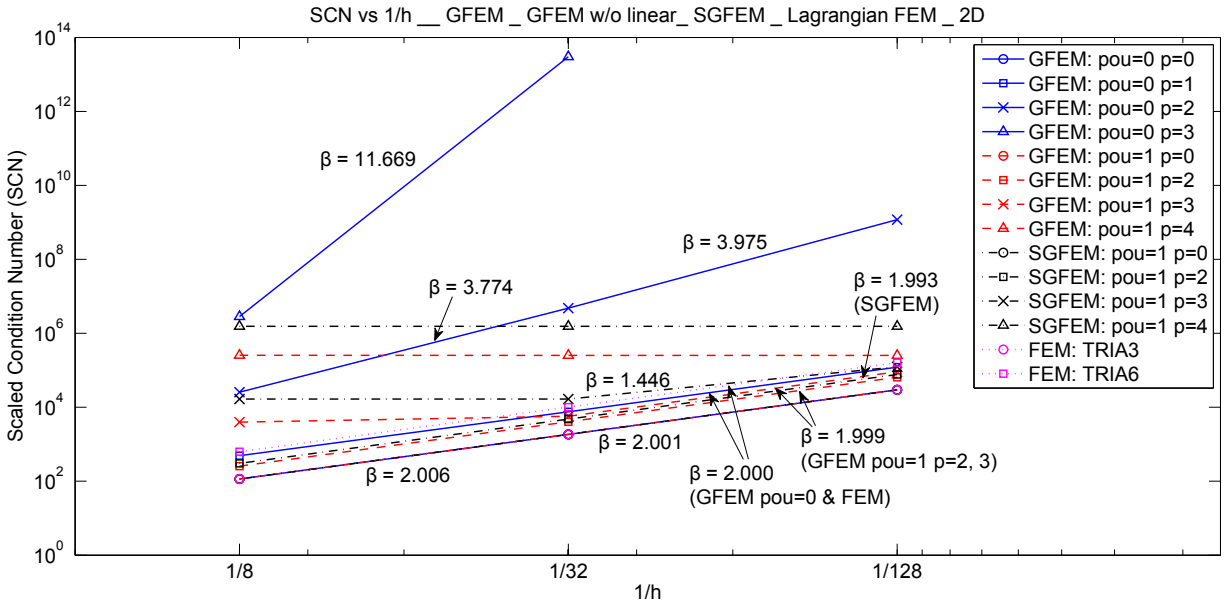


Fig. 3.3 SCN with respect to element size for GFEM (*M2*), GFEM without linear enrichments (*M3*), SGFEM (*M4*), and FEM (*M1*) in 2D

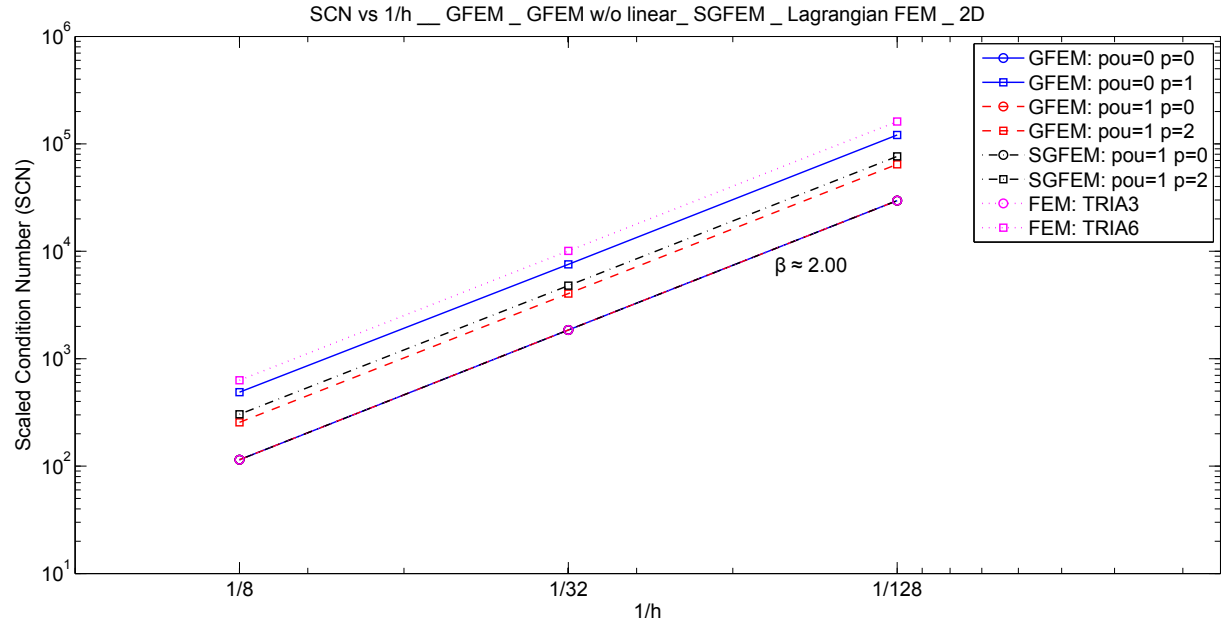


Fig. 3.4 SCN with respect to element size for GFEM (*M2*), GFEM without linear enrichments (*M3*), SGFEM (*M4*), and FEM (*M1*) in 2D for low *p*-order

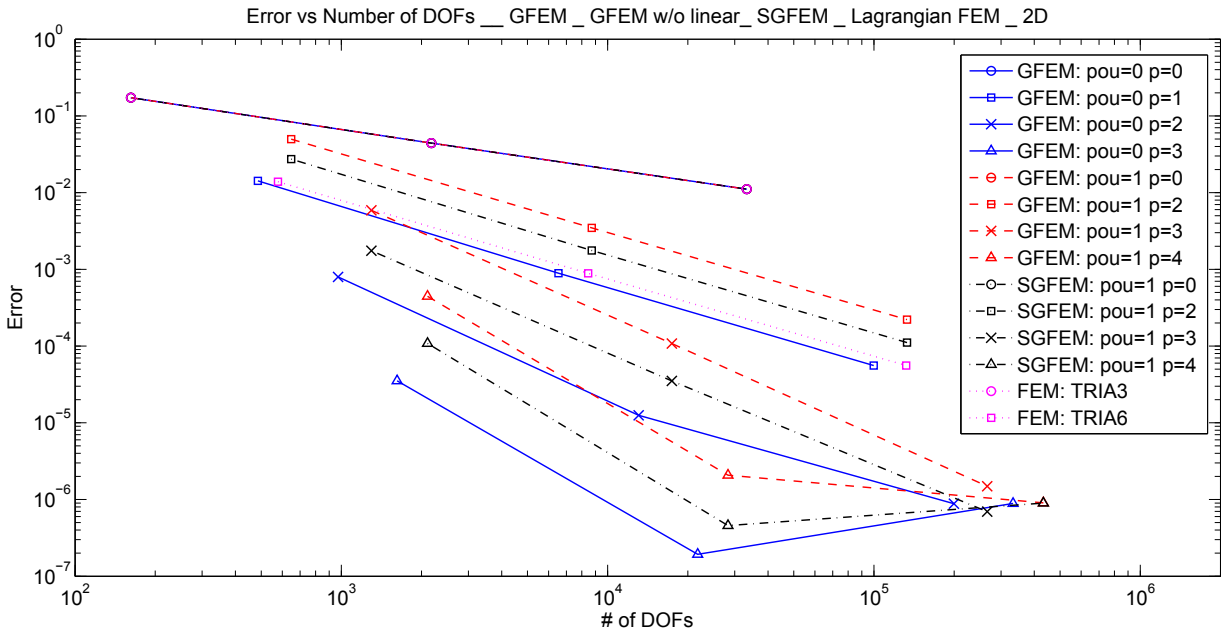


Fig. 3.5 Relative error in energy norm with respect to number of DOFs for GFEM (*M2*), GFEM without linear enrichments (*M3*), SGFEM (*M4*), and FEM (*M1*) in 2D

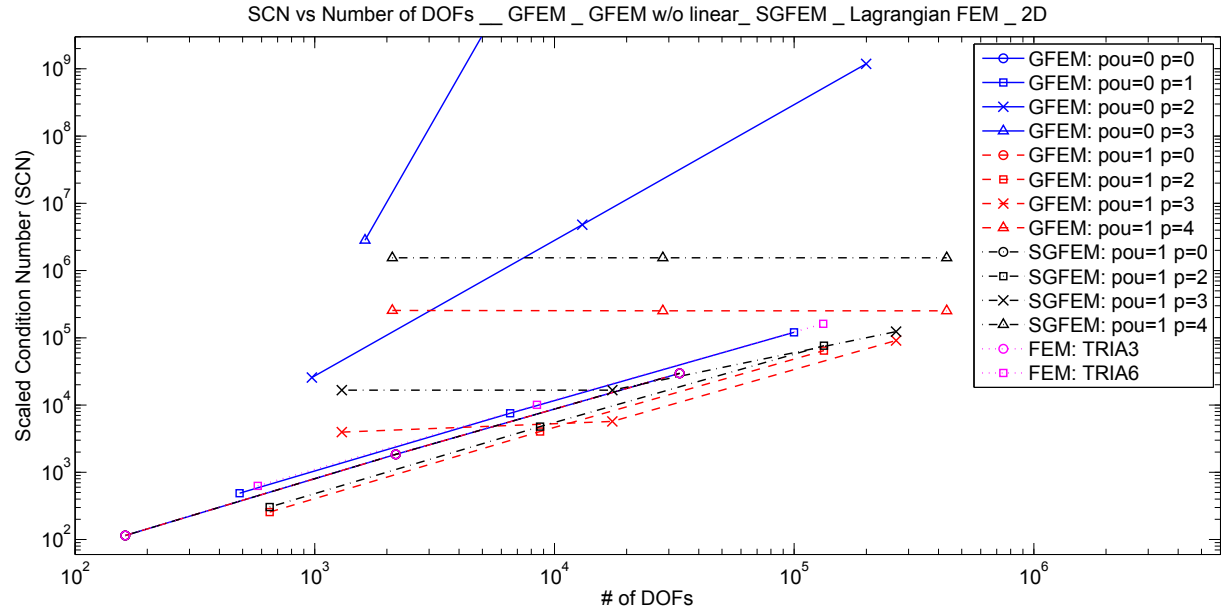


Fig. 3.6 SCN with respect to number of DOFs for GFEM (*M2*), GFEM without linear enrichments (*M3*), SGFEM (*M4*), and FEM (*M1*) in 2D

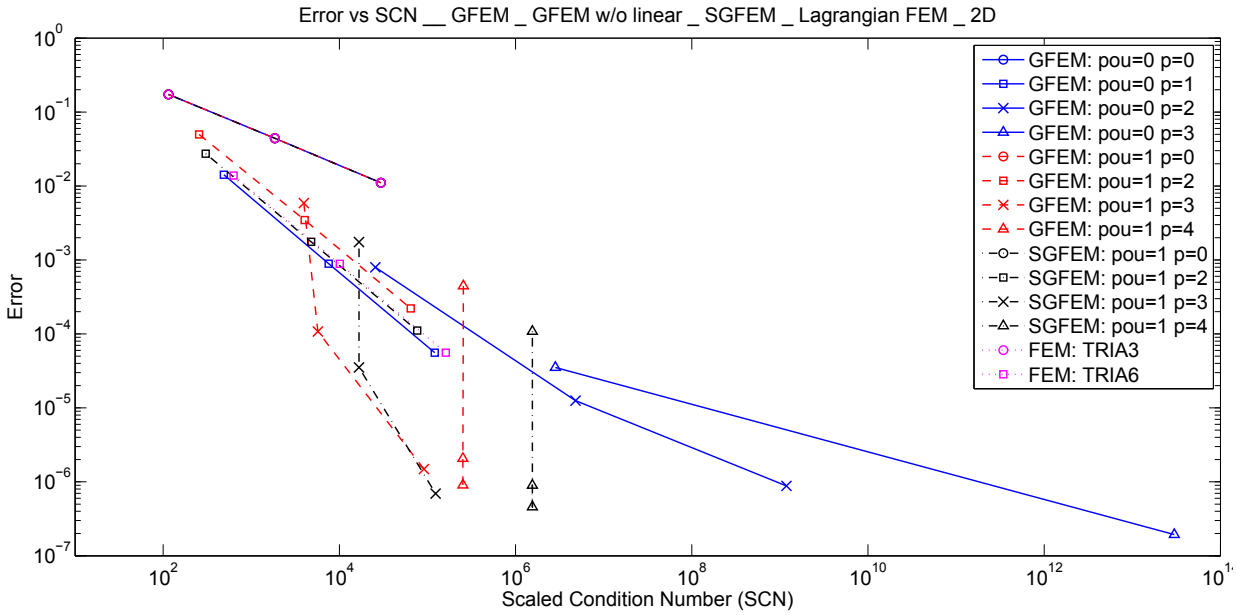


Fig. 3.7 Relative error in energy norm with respect to SCN for GFEM (*M2*), GFEM without linear enrichments (*M3*), SGFEM (*M4*), and FEM (*M1*) in 2D

Table 3.1 First few eigenvalues and the largest eigenvalues (indicated in square bracket) for FEM (*M1*) The multiplicity of zero eigenvalues is indicated in bracket unless it is equal to one

h	8x8	32x32	128x128
TRIA3	0(3)	0(3)	0(3)
	2.7136e-02	1.6826e-03	1.0507e-04
	3.1822e-02	2.0343e-03	1.2726e-04
	3.3203e-02	2.0397e-03	1.2728e-04
	3.4826e-02	2.1463e-03	1.3388e-04
	[3.111111]	[3.111111]	[3.111111]
TRIA6	0(3)	0(3)	0(3)
	5.3919e-03	3.3626e-04	2.1014e-05
	6.4334e-03	4.0693e-04	2.5452e-05
	6.4349e-03	4.0693e-04	2.5452e-05
	6.8434e-03	4.2832e-04	2.6773e-05
	[3.394004]	[3.393872]	[3.393860]

Table 3.2 First few eigenvalues and the largest eigenvalues (indicated in square bracket) for GFEM (*M2*) The multiplicity of zero eigenvalues is indicated in bracket unless it is equal to one

p=0	0(3)	0(3)	0(3)
	2.7136e-02	1.6826e-03	1.0507e-04
	3.1822e-02	2.0343e-03	1.2726e-04
	3.3203e-02	2.0397e-03	1.2728e-04
	3.4826e-02	2.1463e-03	1.3388e-04
	[3.111111]	[3.111111]	[3.111111]
p=1	0(9)	0(9)	0(9)
	1.0012e-02	6.4708e-04	4.0465e-05
	1.0246e-02	6.4836e-04	4.0611e-05
	1.5934e-02	1.0162e-03	6.3571e-05
	1.8805e-02	1.2054e-03	7.5447e-05
	[4.890717]	[4.890712]	[4.890687]
p=2	0(19)	0(19)	0(19)
	3.2658e-04	1.7441e-06	7.0537e-09
	3.6543e-04	1.8643e-06	7.4267e-09
	7.7851e-04	4.3479e-06	1.7599e-08
	9.2288e-04	5.2348e-06	2.1144e-08
	[8.363083]	[8.363007]	[8.362944]
p=3	0(33)	0(33)	
	4.2444e-06	4.0005e-13	
	4.4826e-06	1.7642e-09	
	1.1723e-05	4.1483e-09	
	1.3453e-05	5.1273e-09	
	[11.988559]	[11.988558]	

Table 3.3 First few eigenvalues and the largest eigenvalues (indicated in square bracket) for GFEM without linear enrichments (*M3*)
The multiplicity of zero eigenvalues is indicated in bracket unless it is equal to one

h	8x8	32x32	128x128
p=0	0(3)	0(3)	0(3)
	2.7136e-02	1.6826e-03	1.0507e-04
	3.1822e-02	2.0343e-03	1.2726e-04
	3.3203e-02	2.0397e-03	1.2728e-04
	3.4826e-02	2.1463e-03	1.3388e-04
	[3.111111]	[3.111111]	[3.111111]
p=2	0(3)	0(3)	0(3)
	2.6516e-02	1.6794e-03	1.0506e-04
	2.9497e-02	2.0237e-03	1.2722e-04
	2.9654e-02	2.0244e-03	1.2722e-04
	3.2852e-02	2.1363e-03	1.3384e-04
	[6.784978]	[6.782371]	[6.782199]
p=3	0(3)	0(3)	0(3)
	2.4251e-03	1.6793e-03	1.0506e-04
	2.4251e-03	2.0233e-03	1.2722e-04
	2.6332e-03	2.0241e-03	1.2722e-04
	2.6332e-03	2.1362e-03	1.3384e-04
	[9.584889]	[9.584872]	[9.584688]
p=4	0(3)	0(3)	0(3)
	5.5496e-05	5.6055e-05	5.6059e-05
	5.6240e-05	5.6055e-05	5.6059e-05
	5.9952e-05	6.0560e-05	6.0565e-05
	6.0769e-05	6.0560e-05	6.0565e-05
	[14.156273]	[14.156213]	[14.156148]

Table 3.4 First few eigenvalues and the largest eigenvalues (indicated in square bracket) for SGFEM (*M4*) The multiplicity of zero eigenvalues is indicated in bracket unless it is equal to one

h	8x8	32x32	128x128
p=0	0(3)	0(3)	0(3)
	2.7136e-02	1.6826e-03	1.0507e-04
	3.1822e-02	2.0343e-03	1.2726e-04
	3.3203e-02	2.0397e-03	1.2728e-04
	3.4826e-02	2.1463e-03	1.3388e-04
	[3.111111]	[3.111111]	[3.111111]
p=2	0(3)	0(3)	0(3)
	2.6429e-02	1.6794e-03	1.0506e-04
	2.9059e-02	2.0236e-03	1.2722e-04
	2.9471e-02	2.0243e-03	1.2722e-04
	3.2853e-02	2.1363e-03	1.3384e-04
	[8.036369]	[8.033615]	[8.033410]
p=3	0(3)	0(3)	0(3)
	7.7947e-04	7.7947e-04	1.0506e-04
	7.7947e-04	7.7947e-04	1.2722e-04
	1.0019e-03	1.0018e-03	1.2722e-04
	1.0019e-03	1.0018e-03	1.3384e-04
	[12.997064]	[12.997064]	[12.996731]
p=4	0(3)	0(3)	0(3)
	1.4758e-05	1.4764e-05	1.4765e-05
	1.4763e-05	1.4764e-05	1.4765e-05
	1.5531e-05	1.5541e-05	1.5543e-05
	1.5540e-05	1.5541e-05	1.5543e-05
	[22.865305]	[22.865298]	[22.864236]

3.4 Mesh perturbation

In the following section, the interior nodes of the mesh are perturbed randomly yet within some control. The nodes on the domain boundary are not perturbed. The perturbation is performed in the following way.

The distorted values in x and y directions at one node are denoted by Δx and Δy which read

$$\Delta x = (r_1 \alpha h)\ cos(2\pi\ r_2) \tag{3.14}$$

$$\Delta y = (r_1 \alpha h)\ sin(2\pi\ r_2) \tag{3.15}$$

In the above expressions, h is the size of the element. α indicates the ratio of the maximum perturbed value in each direction at each node and the element size. It is for preventing extremely distorted elements in the mesh. r_1 and r_2 are two random numbers generated by the machine and scaled by the largest random number (i.e., $r_1,\ r_2 \in [0,1]$). These two random numbers vary from node to node. Thus, different interior nodes are perturbed with different values. In this study, we set the perturbation parameter $\alpha = 0.3$.

Therefore, the perturbed coordinates of the interior nodes are given by

$$\tilde{x} = x + \Delta x \tag{3.16}$$

$$\tilde{y} = y + \Delta y \tag{3.17}$$

where $\tilde{x}$ and $\tilde{y}$ are the nodal coordinates after perturbation, and x and y are the nodal coordinates before perturbation.

Figures 3.8, 3.9, 3.10, and 3.11 illustrate errors and conditioning results for TRIA6 and the standard SGFEM before and after perturbation of the interior mesh points. The same distorted meshes are used for both methods. Figure 3.12 shows an example of a distorted 8x8 mesh. The plots show that both FEM and SGFEM are stable under perturbation. Errors and condition numbers remain nearly the same as for the undistorted mesh. The standard SGFEM is less sensitive than FEM in terms of the error under mesh perturbation.

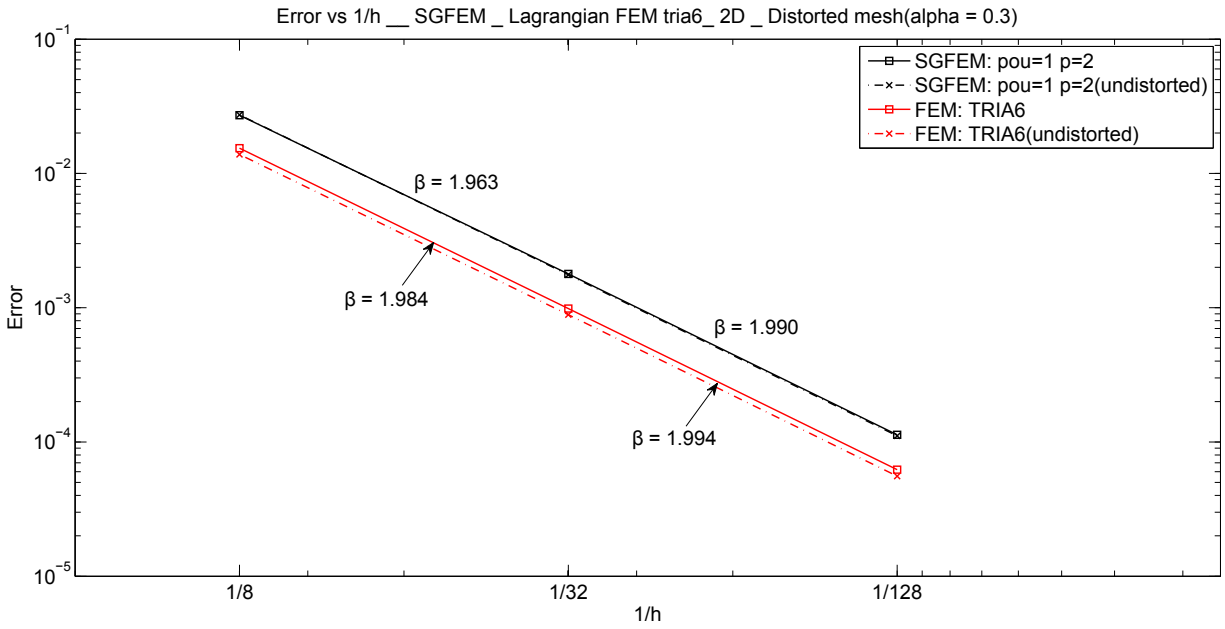


Fig. 3.8 Relative error in energy norm with respect to element size for SGFEM (*M4*) and TRIA6 (*M1*) with perturbation parameter $\alpha = 0.3$

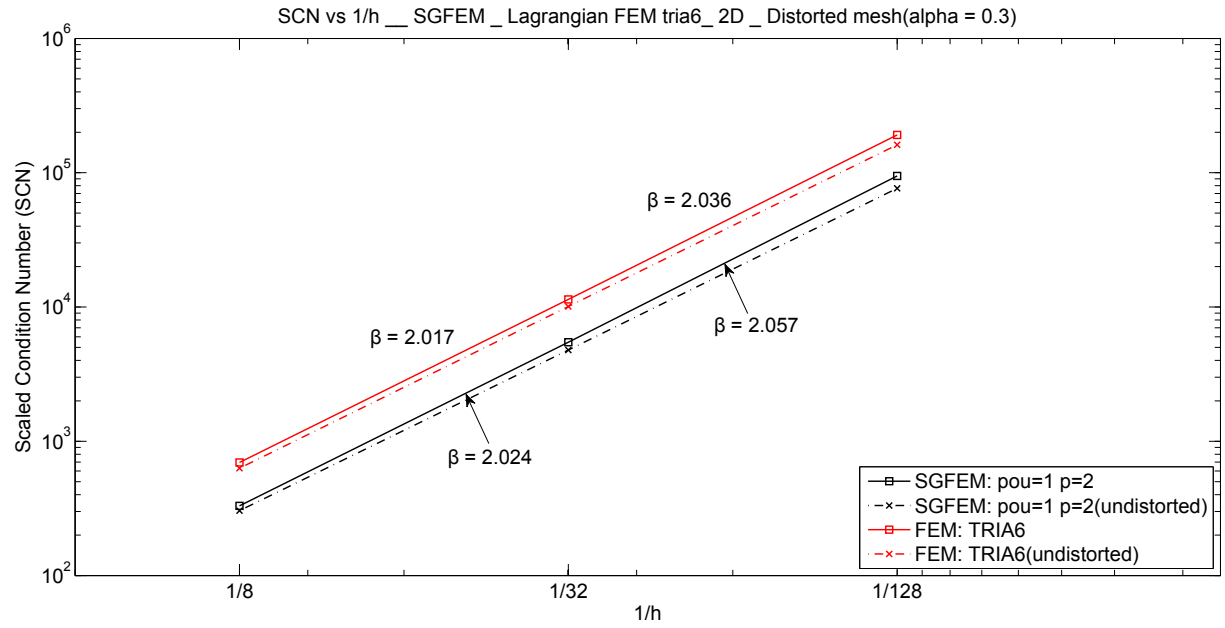


Fig. 3.9 Scaled condition number with respect to element size for SGFEM (*M4*) and TRIA6 (*M1*) with perturbation parameter $\alpha = 0.3$

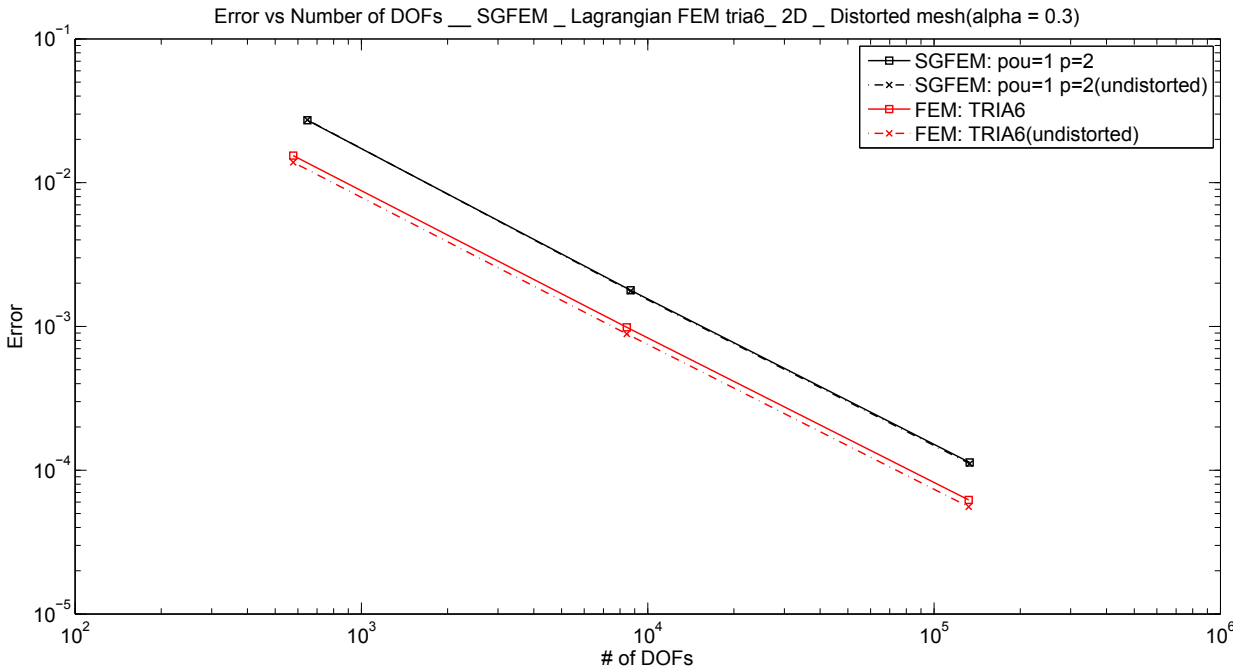


Fig. 3.10 Relative error in energy norm with respect to DOFs for SGFEM (*M4*) and TRIA6 (*M1*) with perturbation parameter $\alpha = 0.3$

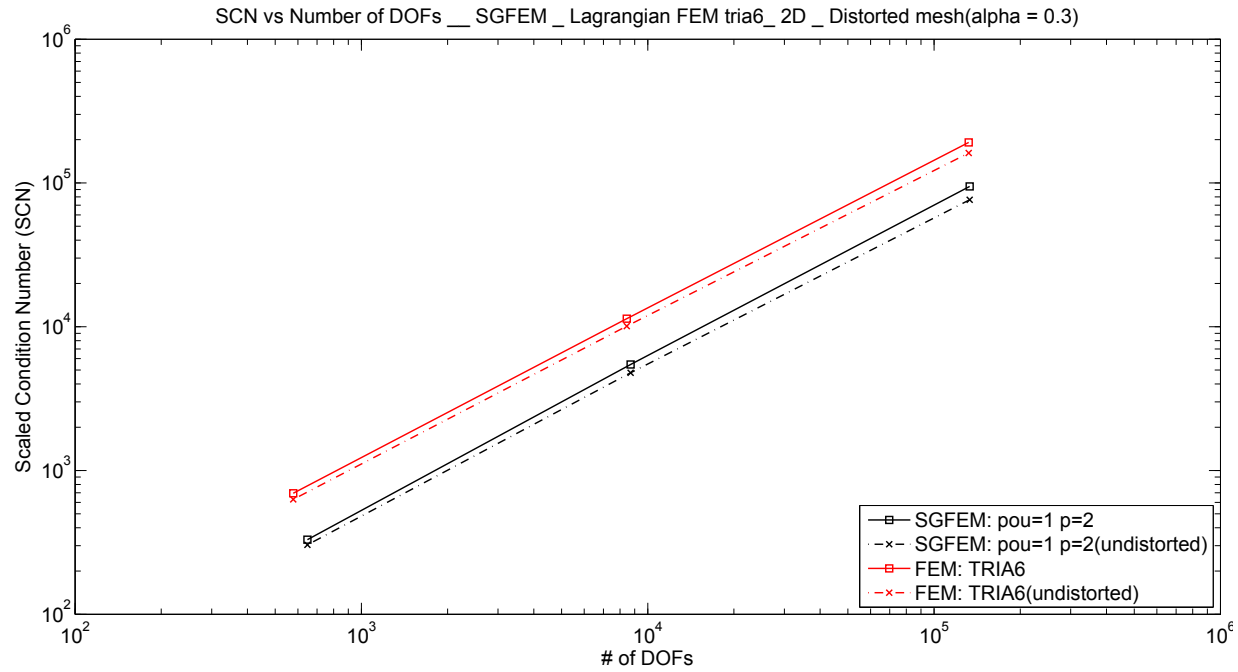


Fig. 3.11 Scaled condition number with respect to DOFs for SGFEM (*M4*) and TRIA6 (*M1*) with perturbation parameter $\alpha = 0.3$

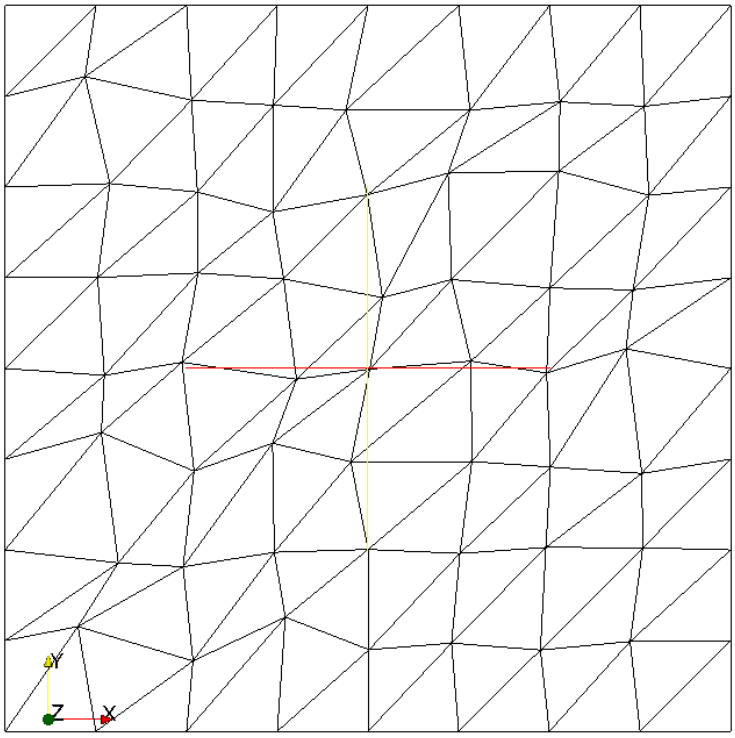


Fig. 3.12 Distorted mesh 8x8 with $\alpha = 0.3$

3.5 Numerical Expense: factorization time

Another comparison we can make between methods is the processing time taken to solve the problem. In the following section, Total DOFs and the left-hand side (LHS) factorization time of TRIA6, standard GFEM, and standard SGFEM are plotted with the error in energy norm being the vertical axis in Figures 3.13 and 3.14. The solver used for getting the factorization time is the *Pardiso* solver [19, 20, 21, 22]. From these plots, one can observe the efficiency of each method. When making the plot, methods with the same convergence rates are selected. Namely, FEM with TRIA6, GFEM with $pou = 0$ and $p = 1$, and SGFEM with $pou = 1$ and $p = 2$ are investigated in this section.

The plots show that the systems associated with TRIA6 and standard SGFEM discretizations have more DOFs than by the standard GFEM. On the other hand, the factorization time for TRIA6 and GFEM are almost identical, and the LHS formed by SGFEM is slower to get factorized. However, from previous analysis, SGFEM has better conditioning, and the other two methods provide lower errors. Combining all these point, one should select discretization methods according to the problem to solve and research goals. In general, the standard SGFEM is recommended. Although its numerical cost is higher, the conditioning will not spoil the accuracy of the solutions for large problem which is usually the case in the engineering practice. In the case of quadratic approximations, GFEM with $pou = 0$ and $p = 1$ is more efficient than TRIA6 and SGFEM with $p = 2$, while having a conditioning very close to the SGFEM case.

3.6 Summary for 2-D Numerical Experiment

In this chapter, 2-D analysis with the FEM, high-order standard GFEM, GFEM without linear enrichments, and standard SGFEM are performed to solve a BVP with a smooth solutions. The accuracy and conditioning have been studied for all four discretization methods. The behavior on distorted meshes for TRIA6 and standard SGFEM and the LHS factorization time of methods are studied as well. In summary, 2-D analysis gives similar conclusions as 1-D analysis which can be stated as follows.

1. In terms of accuracy, the FEM and standard GFEM provide the lowest error among all methods. GFEM without linear enrichments is the worst accurate and standard SGFEM is in between. The convergence behaviors in 2-D are the same as in 1-D case. The standard GFEM yields the rate of convergence equal to the enrichment order plus one (i.e., $\beta = p + 1$), while

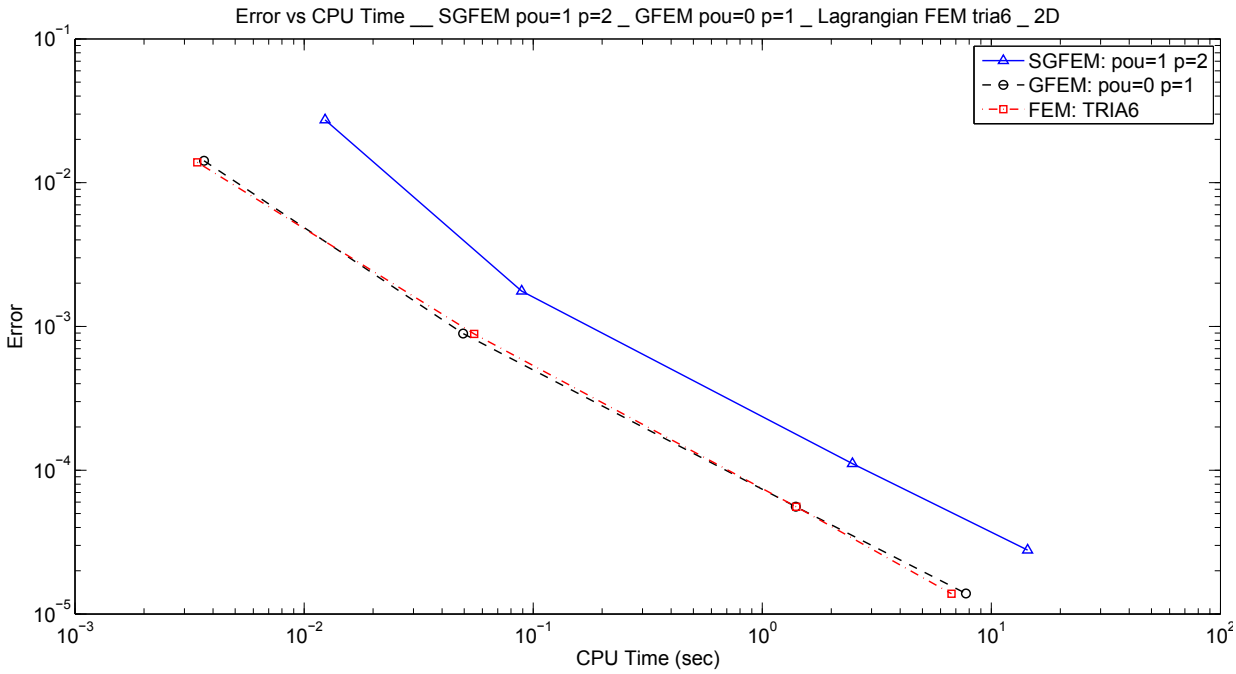


Fig. 3.13 Error in energy norm with respect to LHS factorization time for TRIA6 (*M1*), GFEM (*M2*), and SGFEM (*M4*)

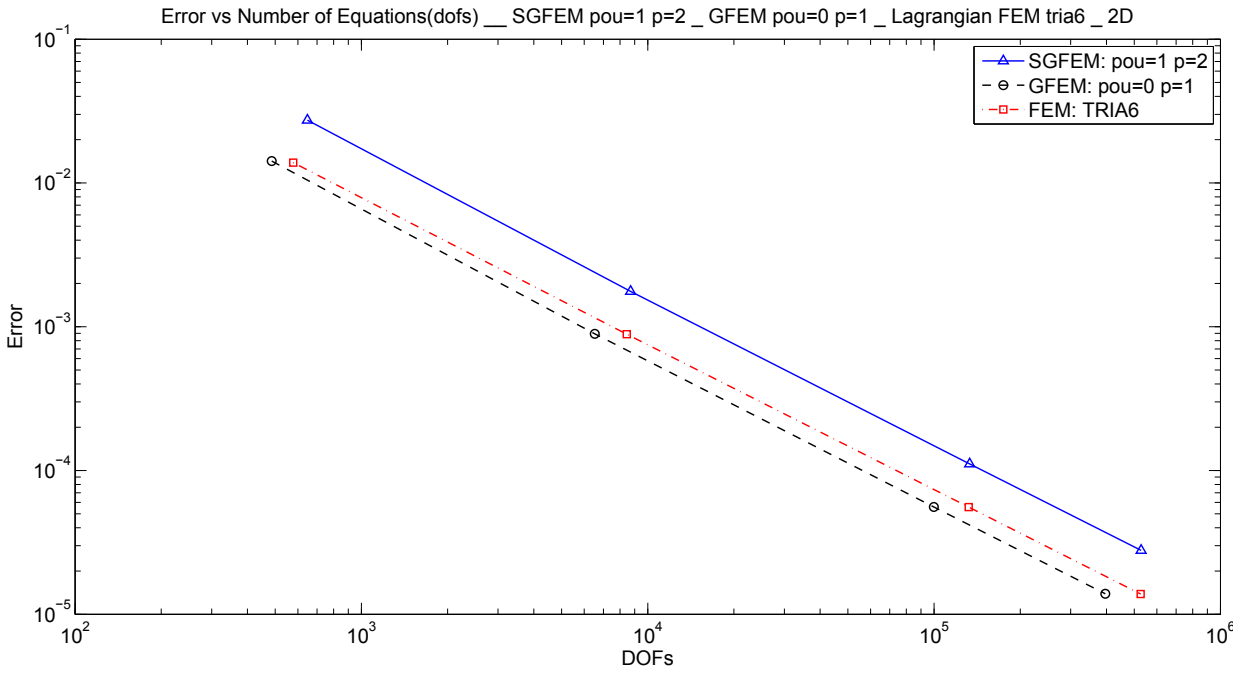


Fig. 3.14 Error in energy norm with respect to total degrees of freedom for TRIA6 (*M1*), GFEM (*M2*), and SGFEM (*M4*)

GFEM without linear enrichments and SGFEM yield the rate of convergence equal to the enrichment order (i.e., $\beta = p$).

2. In terms of conditioning, GFEM without linear enrichments yields the best conditioning behavior as we increase the order and refine the mesh. The standard SGFEM gives a bit larger scaled condition number (SCN) than GFEM without linear enrichment but remains stable during the mesh refinement. For the case of GFEM with linear enrichments (i.e., the standard GFEM), the SCN grows at the same rate as the standard SGFEM and GFEM without linear enrichments. While the SCN for the standard GFEM grows rapidly for quadratic or higher order enrichments meaning that its conditioning is not stable.

3. From the above two points, we observe that once a method provides higher accuracy its conditioning will behave worse. On the other hand, if one method yields stable and small SCN, its accuracy will be lower. This observation matches the behaviors of standard GFEM, SGFEM, and GFEM without linear enrichment in 1-D case.

4. The GFEM without linear enrichments and SGFEM are able to fix the LD issue and eliminate spurious modes of the structure leaving only three zero eigenvalues of the stiffness matrix which denote the rigid body motions in 2-D.

5. For FEM and standard SGFEM, the accuracy and conditioning are not sensitive to the mesh distortion. Between these two methods, SGFEM is less sensitive in terms of errors.

6. As for factorization time, it takes longer to factorize the LHS formed by standard SGFEM than by FEM and standard GFEM.

CHAPTER 4

CONCLUSIONS

This report is focused on comparing the quality of approximation between different discretization methods including *p*-FEM, GFEM, SGFEM, and several modified methods based on standard GFEM and SGFEM. GFEMs and SGFEMs are always constructed based on polynomial enrichments. Both 1-D and 2-D problems solved have smooth solutions. So that each methods can achieve optimal convergence. The FEMs are acting as reference methods. The GFEMs and SGFEMs are the methods of interest. Since the implementation for 1-D case in easier than for 2-D case, nine methods are investigated for 1-D problem while four of them are studied for 2-D case. Some conclusions drawn from the 1-D numerical experiment can be reinforced by the results of the 2-D experiment. Throughout the report, we perform the study on the discretization methods with respect to the accuracy, the convergence rate, the conditioning, the LD issue, the factorization cost, and the behavior against mesh perturbation. To summarize all remarks from 1-D and 2-D BVPs, the conclusions about GFEM family methods can be stated as follow.

1. **Accuracy and conditioning**

   The accuracy and conditioning have opposite behaviors when we switch from one method to another. In other words, once a modification on discretization formulation causes improvement in accuracy, the conditioning of this method will be degraded. The aspects that affect the behavior include the completeness of the enrichment, the subtraction of the FE interpolants, and the use of shifting in the enrichment. Skipping the linear enrichments (i.e., from *M3* to *M4*, from *M6* to *M5* in 1-D, and from *M2* to *M3* in 2-D) leads to stabilized conditioning but lower accuracy. Subtracting the FE interpolants (i.e., from *M4* to *M5* in 1-D, and from *M3* to *M4* in 2-D) will provide improvement in accuracy and stable yet larger condition numbers. The use of shifting (i.e., from *M9* to *M8* in 1-D) can stabilize the conditioning of the stiffness matrix. Additionally, the use of scaling (i.e., from *M5* to *M9* in 1-D) may also affect the accuracy of the approximation due to the precision in representing the geometry.

2. **Convergence**

   From the numerical experiments performed, the rates of convergence are determined by the

completeness of the enrichments. For standard GFEM (i.e., *M3* in 1-D and *M2* in 2-D) and SGFEM Mod2 (i.e., *M6* in 1-D), a complete set of polynomial enrichments is adopted. The resulting convergence rate is equal to the enrichment order plus one (i.e., $\beta = p + 1$) for problems with smooth solutions. Skipping one level of terms in the enrichments (i.e., *M4*, *M5*, and *M7* in 1-D, *M3* and *M4* in 2-D) will not lead a jump in the convergence rate according to the next order of enrichments. As a result, the rates of convergence after skipping linear or quadratic enrichments will be equal to the enrichment order p. In addition, both scaling and shifting have no influence on the convergence behavior.

3. **The linear dependency (LD) issue**

   The LD issue can be fixed by skipping terms in the enrichments. All methods investigated in this report that have complete polynomial enrichments (i.e., *M3* and *M6* in 1-D, *M2* in 2-D) are suffering the LD issue. Some spurious modes exist in the resulting system. Meanwhile, the LD issue is usually accompanied with bad conditioning. On the other hand, the absence of the linear enrichments (i.e., *M4* and *M5* in 1-D, *M3* and *M4* in 2-D) can fix the LD issue and lead to good conditioning at the same time. The absence of the quadratic enrichment (i.e., *M7* in 1-D) can eliminate some yet not all spurious modes and also stabilize the condition numbers. The LD is not affected by the scaling or shifting.

4. **Mesh perturbation**

   The FEM and standard SGFEM are both insensitive to the distortion of the mesh. By comparing, the standard SGFEM is less sensitive than the FEM when the interior nodes of the mesh are perturbed.

5. **Numerical cost**

   As compared to the FEM and standard GFEM, the system formed by the standard SGFEM requires longer time to be factorized. The factorization time spent on processing the system formed by standard GFEM is comparable to that for FEM. For problems with a large number of DOFs, GFEM might be numerically economical. However, the user should keep in mind that the conditioning for standard GFEM becomes even worse for large problems which could possibly spoil the accuracy of the solution, while the standard SGFEM provides good conditioning. Therefore, one needs to balance the numerical cost and the approximation quality before performing the experiment.

Based on the observations and remarks in this thesis, the readers and the users of GFEM family methods can choose appropriate discretization methods according to their research objects. Moreover, provided in this report the effects of each type of modifications, one can also construct other

modified versions of Generalized Finite Element methods that can yield desirable approximation qualities.

REFERENCES

[1] J. T. Oden, C. A. M. Duarte, and O. C. Zienkiewicz, A new cloud-based *hp* finite element method, *Computer Methods in Applied Mechanics and Engineering*, vol. 153, no. 12, pp. 117 – 126, 1998.

[2] C. A. Duarte and J. T. Oden, *Hp* cloudsan *hp* meshless method, *Numerical Methods for Partial Differential Equations*, vol. 12, pp. 673–705, 1996.

[3] I. Babuška and J. M. Melenk, The partition of unity method, *International Journal for Numerical Method in Engineering*, vol. 40, pp. 727–758, 1997.

[4] J. M. Melenk and I. Babuška, The partition of unity finite element method: Basic theory and applications, *Computer Methods in Applied Mechanics and Engineering*, vol. 139, pp. 289 – 314, 1996.

[5] C. A. Duarte, I. Babuška, and J. T. Oden, Generalized finite element methods for three-dimensional structural mechanics problems, *Computers & Structures*, vol. 77, no. 2, pp. 215 – 232, 2000.

[6] J. Kim and K.-J. Bathe, The finite element method enriched by interpolation covers, *Computers & Structures*, vol. 116, no. 0, pp. 35 – 49, 2013.

[7] R. Tian, G. Yagawa, and H. Terasaka, Linear dependence problems of partition of unity-based generalized fems, *Computer Methods in Applied Mechanics and Engineering*, vol. 195, pp. 4768 – 4782, 2006.

[8] R. Tian, Extra-dof-free and linearly independent enrichments in GFEM, *Computer Methods in Applied Mechanics and Engineering*, vol. 266, no. 0, pp. 1 – 22, 2013.

[9] X. M. An, L. X. Li, G. W. Ma, and H. H. Zhang, Prediction of rank deficiency in partition of unity-based methods with plane triangular or quadrilateral meshes, *Computer Methods in Applied Mechanics and Engineering*, vol. 200, no. 58, pp. 665 – 674, 2011.

[10] X. M. An, Z. Y. Zhao, H. H. Zhang, and L. X. Li, Investigation of linear dependence problem of three-dimensional partition of unity-based finite element methods, *Computer Methods in Applied Mechanics and Engineering*, vol. 233236, no. 0, pp. 137 – 151, 2012.

[11] H. Li, A note on the conditioning of a class of generalized finite element methods, *Applied Numerical Mathematics*, vol. 62, no. 6, pp. 754 – 766, 2012.

[12] Y. Cai, X. Zhuang, and C. Augarde, A new partition of unity finite element free from the linear dependence problem and possessing the delta property, *Computer Methods in Applied Mechanics and Engineering*, vol. 199, no. 1720, pp. 1036 – 1043, 2010.

[13] I. Babuška and U. Banerjee, Stable generalized finite element method (SGFEM), *Computer Methods in Applied Mechanics and Engineering*, vol. 201204, no. 0, pp. 91 – 111, 2012.

[14] Q. Zhang, U. Banerjee, and I. Babuška, Higher order stable generalized finite element method, *Numerische Mathematik*, pp. 1–29, 2014.

[15] V. Gupta, C. A. Duarte, I. Babuška, and U. Banerjee, A stable and optimally convergent generalized FEM (SGFEM) for linear elastic fracture mechanics, *Computer Methods in Applied Mechanics and Engineering*, vol. 266, no. 0, pp. 23 – 39, 2013.

[16] B. Szabó and I. Babuška, *Finite Element Analysis*. John Wiley & Sons, Inc., New York, 1991.

[17] C.-G. Kim and J. Park, The condition number of stiffness matrix under p-version of the FEM, *Kangweon-Kyungki Mathematical Journal*, vol. 6, pp. 17–26, 1998.

[18] B. Szabó, A. Düster, and E. Rank, The p-version of the finite element method, *Encyclopedia of Computational Mechanics (Chapter 5)*, 2004.

[19] *Intel® Math Kernel Library User's Guide*. Intel Corporation.

[20] A. Kuzmin, M. Luisier, and O. Schenk, Fast methods for computing selected elements of the green's function in massively parallel nanoelectronic device simulations, in *Euro-Par 2013 Parallel Processing*, ser. Lecture Notes in Computer Science, F. Wolf, B. Mohr, and D. Mey, Eds. Springer Berlin Heidelberg, 2013, vol. 8097, pp. 533–544.

[21] O. Schenk, M. Bollhoefer, and R. A. Roemer, On large scale diagonalization techniques for the anderson model of localization, *SIAM Journal on Scientific Computing*, vol. 28, pp. 963–983, 2006.

[22] O. Schenk, A. Wächter, and M. Hagemann, Matching-based preprocessing algorithms to the solution of saddle-point problems in large-scale nonconvex interior-point optimization, *Computational Optimization and Applications*, vol. 36, no. 2-3, pp. 321–341, 2007.